Max Planck Institüt für Kolloid- und Grenzflächenforschung
Arbeitsgruppe Prof. Dr. Reinhard Lipowsky

Interactions of Functionalized Vesicles in the Presence of Europium (III) Chloride

Dissertation
zur Erlangung des akademischen Grades
"doctor rerum naturalium"
(Dr. rer. nat.)
in der Wissenschaftsdisziplin Experimentelle Physik

eingereicht an der
Mathematisch-Naturwissenschaftlichen Fakultät
der Universität Potsdam

von
Christopher K. Haluska

Potsdam im Oktober 2004

Abstract

We incorporate amphiphilic receptors bearing ß-diketone functional units into large (LUV's) and giant unilamellar vesicles (GUV's). Electrolyte solutions containing di- and trivalent ions were used to induce inter-membrane interactions. Measurements performed with isothermal titration calorimetry (ITC) revealed that interaction between $EuCl_3$ and ß-diketone receptors was characterized by a molar enthalpy 126 ± 5 kcal/mole and an equilibrium binding constant 26 ± 4 mM^{-1}. The results indicate a molecular complex formed binding two ß-diketone receptors to one Eu^{3+} ion. Dynamic light scattering (DLS) was used to follow changes in LUV diameter indicated in an increase in vesicle size distribution of on average 20 %. Optical microscopy was employed to visualize the inter-membrane interaction measured using DLS and ITC. Depending on membrane composition of the functionalized vesicles we found that local injections of micromolar $EuCl_3$ induced membrane pore formation and membrane fusion. Our collection of results leads to the conclusion that formation of intra-molecular ligand receptor complexes leads to pore formation and inter-membrane complex formation leads to membrane fusion. Detailed characterization of the fusion process shows that irreversible opening of the fusion pore can be extrapolated to times below 50 μsec. We have found that formation of membrane bound ligand (Eu^{3+})-receptor complexes provides versatility to the function of vesicle membranes.

I. Introduction

Fusion of membranes, an essential cellular process is rather complex and remains poorly understood. In the last twenty to thirty years biologist and physicists have been working independently, and cooperatively, to solve the mystery of membrane fusion (Lentz, Malinin et al. 2000; Jahn and Grubmüller 2002; Jahn, Lang et al. 2003; Tamm, Crane et al. 2003). Both theoretical and experimental physics have been applied to investigate pure lipid bilayer systems, and more specifically, the factors that affect fusion of membranes. (Duzgunes, Wilschut et al. 1983; Lee and Lentz 1997; Pantazatos and MacDonald 1999; Markin and Albanesi 2002). In particular the physics of fusion concentrates on barriers and pathways to fused membranes. Biologically based investigations of viral and intracellular systems have uncovered proteins and families of proteins that take part in the fusion of biological membranes. Using results from experiments, simulations, and calculations scientists are trying to piece together a coherent picture which explains the cooperative behavior between proteins and lipids, as well as the individual roles that each plays leading to fusion of two independent membranes (Jahn and Grubmüller 2002; Jahn, Lang et al. 2003; Tamm, Crane et al. 2003).

Membrane fusion, the merger between two separate membranes resulting in the complete mixing of different compartments, is thought to proceed through a pathway containing a number of intermediate steps (Figure I-1). This pathway is thought to include events such as membrane contact or docking, and proximal monolayer mixing, leading to the formation of a membrane stalk. In some cases stalk formation followed by hemifusion of two bilayers, a formation where the distal monolayers are thought to form a transient bilayer that prevents the exchange of contents between the two separate compartments. The hemifused diaphragm would be the thinnest object separating the two internal volumes, allowing mixing of only half of the lipids from each membrane. Finally, mixing of lipids leading to formation of a fusion (or lipidic) pore in the bilayer or hemifusion diaphragm, is paramount to the completion of the fusion process. The fusion pore is sometimes observed to be small and transient (reversible), but an abrupt and irreversible pore opening is required to allow for total fusion and complete mixing of the lipids from the two bilayers.

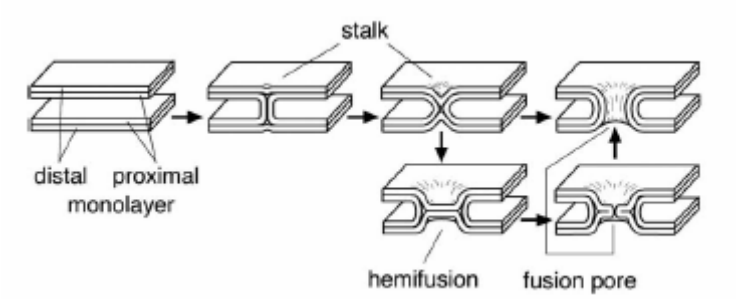

Figure I-1. Fusion Intermediates: The figure illustrates the pathway to membrane fusion and the intermediate membrane structures encountered along the way as predicted by the stalk model. (Jahn, Lang et al. 2003).

While the steps in the membrane fusion (mechanical) pathway detailed above are well studied, it is not absolutely required that all steps are involved in the fusion process. It is agreed upon that there is a certain energy barrier that must be overcome before fusion can occur (Lentz, Malinin et al. 2000). The first obstacle to fusion is membrane contact or docking of membranes. Interference to membrane contact includes factors such as hydration and steric forces. Hydration forces ensure that hydrophilic portions of the amphiphiles are in favorable conditions by forming water layers that keep lipid bilayers stable, independent, and separated in aqueous solutions. Finally, steric forces prevent a physical overlap of bilayers with themselves and of molecules within the bilayers. To surmount any of these factors energy must be added to a given system. In addition, it is not a forgone conclusion that, once membrane contact occurs, fusion will take place.

Details of the intermediate structures, formation of the membrane stalk and the hemifusion diaphragm (also called trans monolayer contact), have been the focus of intense study from a theoretical point of view (Jahn and Grubmüller 2002; Markin and Albanesi 2002). In the eighties a model of the fusion intermediates and calculations of the energies associated with them were put forth in a physical model called the "stalk model" (Kozlov and Markin 1983). Energies associated with the bending of a membrane present the next barrier to fusion in the stalk model. More recently, in the last five years, these models have come under criticism. This has lead to the modification of the models, and recalculation of the energies of the intermediate structures . New calculations have produced an “energy crisis” for the stalk model, leading to predictions ranging from negative kT, a spontaneous process, to up to 200kT, a seemingly unphysical energy for some of the fusion intermediates (Markin and Albanesi 2002). Regardless of the energy calculated for the fusion process it is

agreed upon that the intermediates only present a "rule of thumb" barrier that must be overcome before fusion (of two membranes) takes place.

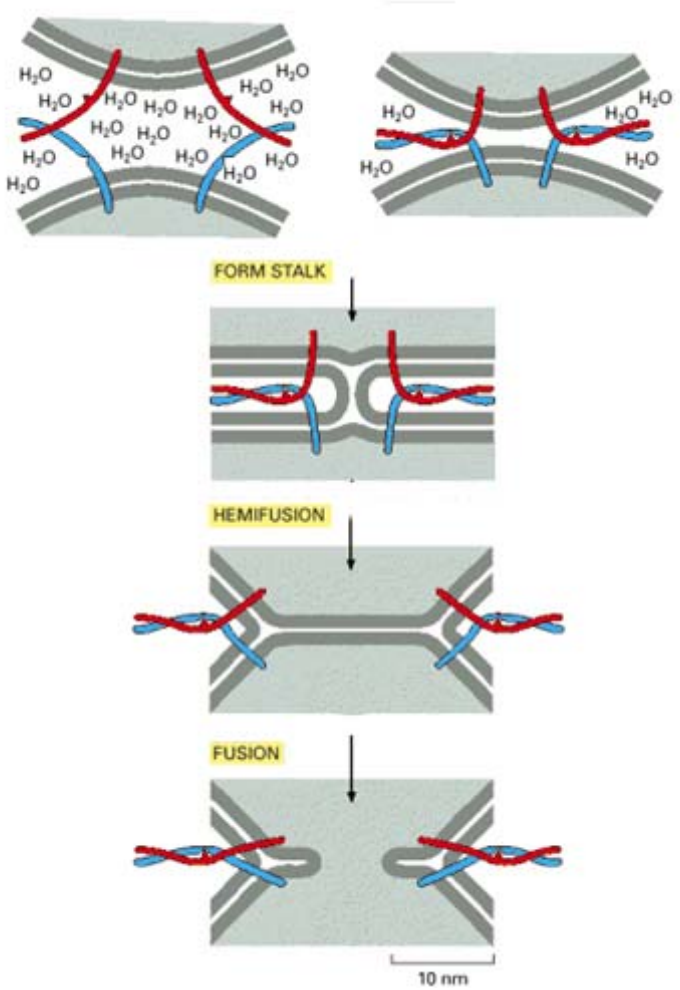

Figure I-2. Proteins in Fusion: This cartoon illustrates the action of SNARE proteins in fusion of biomembranes. The process the same steps as predicted in the stalk model, including docking (top), followed by hemifusion (middle), leading to complete membrane fusion (Alberts, Johnson et al. 2001).

From a biological view point it is thought that proteins provide the energy needed to overcome the barriers primarily the removal of a hydration barrier, demonstrated in Figure I-2. Two current areas of interest regarding fusion of biomembranes are viral fusion and secretory fusion (Lentz, Malinin et al. 2000; Jahn, Lang et al. 2003; Tamm, Crane et al. 2003). Viral fusion involves the action of just one type of protein that acts to induce fusion between two different membranes. Secretory fusion on the other hand involves a number of different proteins that act together to induce the fusion process. In both cases it is thought that a primary function of the proteins is to remove a spatial barrier between target and host membranes. This work is necessary before fusion between membranes can occur.

Once the membranes are together it is unclear whether it is the protein-protein or protein-lipid interaction that results in the fusion of membrane. In some cases it is thought that proteins only catalyze fusion, whereas others propose that fusion proteins act to disrupt the bilayer structure and cause fusion between two membranes. As such the role of fusion proteins is not completely understood.

Given all of the factors preventing membrane fusion, and all of the questions surrounding the process, engineering a system to study events associated with membrane fusion is no easy task. In this work we choose to investigate fusion using a reduced system. By incorporating functionalized amphiphiles into a lipid membrane we aim to induce fusion in a controlled fashion. Once this is achieved, the goal is to characterize the events leading up to and governing the process of membrane fusion.

A. The Cell Membrane

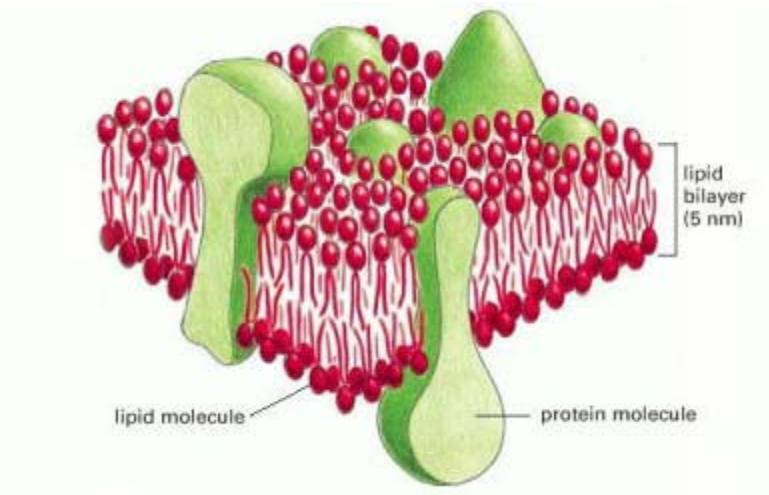

Figure I-3 The Cell Membrane: The figure shows a cartoon of a cell membrane containing both lipids and proteins, two of the main constituents. The figure leaves out a lot of detail but captures the essential features like lipids making up a bilayer membrane and proteins that span the lipid bilayer (Alberts, Johnson et al. 2001).

Biological membranes composed of lipids and proteins, are an absolute necessity for the existence of all forms of life ranging from the largest plants and animals to the smallest single cellular organisms and cell organelles. Membranes enclose everything biological in an organism and the importance of their role increases as one scales down in organizational level from organs, to cells, to cell organelles. Phospholipid membranes scales encompass four orders of magnitude in

length spanning the nanometer (50 nm) and micrometer (100 μm) regimes. With increasing size comes increasing complexity which is typically dependent on the membrane function. In the lab one is able to control membrane complexity independent of size by building model membranes out of only the most essential membrane components.

All cellular and subcellular bodies are composed of various mixtures of lipid, proteins in the form of small and macromolecular assemblies that form supramolecular structures held together by noncovalent interactions. This organization is demonstrated in Figure I-3. Commonly cell organelles contain more than 50 different proteins, and a variety of lipids having various size, shape, and function based on the particular needs of the cellular body. In the laboratory one is able to remove unwanted, irrelevant biological components that may interfere or complicate the system under investigation. This is done by building a model system only from constituents absolutely necessary for investigation of a process. Once this is done, techniques such as nuclear magnetic resonance are applied to determine the structure of the molecules. Additionally neutron or x-ray scattering can also reveal of molecular structure of proteins or membranes. Such methods can furthermore be used to characterize the fundamental membrane properties such as molecular size, area per molecule, and membrane thickness or composition. To work with the most basic system possible, we start by using phospholipids to build model membranes.

B. Lipids

Lipid molecules, primarily phospholipid molecules, form the basis on which cells and cell organelles are constructed. These small cellular bodies derive their function through the operations of protein molecules. The structure of common phospholipids can be broken down in to two main components: an apolar, hydrophobic tail and a polar, hydrophilic head group (Figure I-4). The combination of these components give phospholipids an amphiphilic quality. The chemical composition of phospholipids is defined by its fatty acid chains and a phosphate group found in the tail and head, respectively. A glycerol group provides a bridge that covalently links the fatty acid chains and phosphate group. A phosphate the fatty acid

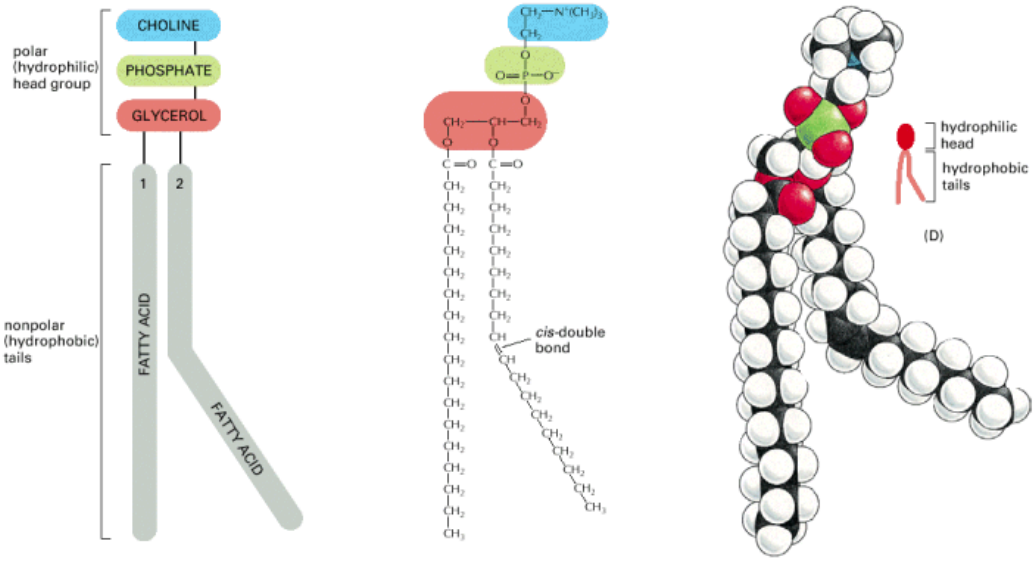

Figure I-4. A Lipid Molecule: Three different representations of a phospholipid molecule; (right to left) a schematic cartoon showing the labeling the different groups and physical properties, an atomistic model showing the atoms and the bonds, and a space filling model, finally a simple representation indicating only the general features of the molecule (Alberts, Johnson et al. 2001).

chains and phosphate group. A phosphate group, the center of the head group, is negatively charged and is bound further to a characterizing moiety that defines the different classes of phospholipids. The three components glycerol, phosphate, and characterizing group make up the hydrophilic portion of the molecule, commonly called the head group.

Two major classes of phospholipids that can be found in common animal cells are phosphatidylcholines (PC), i.e. lecithin, and phosphatidylethanolamines (PE). A unique shape can be associated with each molecule as derived from its molecular structure. The head group is defined by its chemical structure which in terms of its spatial area can also be regarded as an optimal area for a given lipid molecule. In both examples given above the characterizing group contains a positive charge and is integrated into either the choline or ethanolamine moiety. The characterizing group acts to neutralize the negative charge that exists in the phosphate group of a phospholipid. The combination of the negative phosphate group and the positive charge found in PC's and PE's define properties of the head group. The charges present within the molecule cancel each other out and form a neutral head group, but give the phospholipid its polarity with respect to the overall structure of the molecule, and are the determining factor when calculating the optimal area of the head group.

On the other hand, the tails are defined by the length and degree of saturation of the hydrocarbon chains. Phospholipids can have either one or two chains with the hydrocarbon (fatty acid) tail of a phospholipid having, on average, 16 to 18 carbon atoms per chain (Lasic 1993). The number of carbon atoms in the fatty acid tail defines the length of the molecule. The PC's and PE's have two fatty acid chains side by side. In addition, it is often found that one fatty acid chain is unsaturated, as is the case with most PC's, whereas with PE's there are usually two unsaturated bonds per lipid molecule, one in each fatty acid chain. The presence of an unsaturated chain increases the volume occupied by the tail region and affects the thermodynamic properties of the lipid, as well as the packing of molecules in relation to one another. Finally, the statistical average of the hydrocarbon chain conformations can define the length and likewise can one define a volume of the phospholipid.

C. Lipid aggregates

Aggregation of surfactants, in particular lipids, in aqueous solution based on increasing concentration is accurately described using equilibrium thermodynamics. Simple mixing of lipid and water results in lipid assembly in the solution and at interfaces. At an air-water interface the lipids form a monolayer. In solution amphiphiles form aggregates starting from monomers, aggregating into dimers and trimers, leading to micelles and bilayers. The type of aggregate that is formed is strongly influenced by the shape of the lipid, this is illustrated in Figure I-5. The threshold concentration around which aggregation takes place is called the critical aggregation concentration or CAC. Single tail lipids have a higher CAC (10^{-6}M), and form aggregates called micelles. In contrast, double chain lipids, like phospholipids have a much lower CAC (10^{-10} M) and usually form bilayer structures (Figure I-5).

Tanford has been able to describe the aggregation of amphiphiles using the idea of a hydrophobic force, or the hydrophobic effect (Tanford 1980). Aggregation is favorable because it places parts of the amphiphile, especially the hydrophobic parts, in a quasi hydrophobic environment, minimizing the surface area of hydrophobic portions of the amphiphile exposed to the surrounding aqueous solution. Applying the ideas of Tanford and considering the dimensions of a molecule one can take a simpler

approach to predicting the type of aggregate that is formed in solution. The ratio of the volume (v) to the product of optimal head group area (a_o) and critical chain length (l_c) define what is called a critical packing parameter (p).

$$p = \frac{v}{a_o l_c}$$

Application of the packing parameter to define aggregate formation is a simple but effective tool for determining the type of aggregates typically formed in solution.

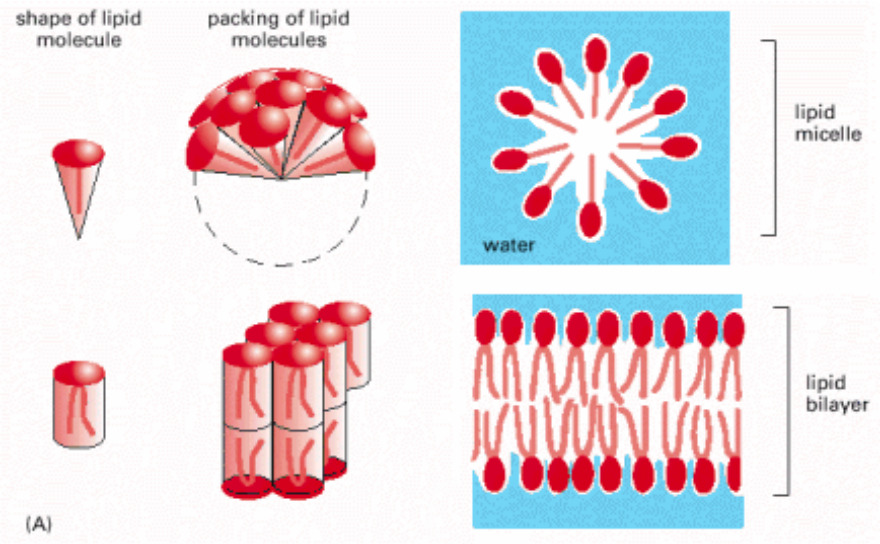

Figure I-5. Lipid Aggregates: The shape and packing of two types of lipid aggregates, micelles (top) and bilayer (bottom). In particular the figure indicates how the number of fatty acid chains reflects the molecular shape and type of aggregate that the lipid will form (Alberts, Johnson et al. 2001).

In solution the smallest aggregates that single chained lipids form are called micelles. These aggregates are small spherical objects with radii approximately equal to the length of a lipid molecule. In the case of infinite lateral (2-D) growth, the aggregate is better described as a membrane with the structure of a bilayer. Those are two different ends of the spectrum, with increasing surfactant concentration the size and shape of the aggregate can also change taking on forms such as long cylinders and discs, so-called worm-like and disk-like micelles, respectively, or closed formed bilayers called liposomes. As well as the concentration, the shape of the molecule also has an impact on the type of aggregate that is formed.

Based on the geometrical arguments given above, the two classes of double-chained lipids mentioned can be shown to take on two different forms, a truncated cone and an inverted cone in the case of the PC's and PE's, respectively (Lasic 1993; Israelachvili 2002). The result is that PC's readily form bilayers, and PE's form what is called an inverted micelle in solution. The membrane bilayer is just the assembly of two separate monolayers. The unique property of the bilayer is its stability in the absence of chemical bonds. In this case the bilayer is held together by noncovalent forces, known as hydrophobic forces. The construction of bilayers is similar to that of micelles, consisting of an apolar hydrophobic core with the polar head groups exposed to the aqueous surfaces. Trapped at the boundary of a substrate the bilayer can remain stable in a planar configuration. Without confining surfaces, and a large line energy on the order of 10^{-6} dyn (10^{-11} J/m) (Harbich and Helfrich 1979), lamellae will become closed structures without edge to limit the exposure of the hydrophobic bilayer core to water. The result is a three-dimensional closed bilayer membrane structure. These closed lipid bodies are called liposomes, or equivalently, vesicles.

Liposomes, assembled from a single type of lipid, serve as model surfaces to study biophysical processes. The bilayer traps a volume of the solvent in its interior. In that way they are like thin lipid bags containing a volume of fluid. Vesicles have long been used as model systems to try to understand more complicated cellular processes. Their size can range from nanometers to tens of microns in diameter. As such they are a useful tool to study critical biological questions in regard to membrane permeability, cellular transport, endo- or exocytosis, mechanical or rheological properties, and fusion of membranes.

Versatility of the vesicle size is one advantage to using vesicles, and a main reason it is used as a model system. In particular, depending on the preparation technique used, it is possible to create a range of vesicles with different sizes and lamellarities. The two different vesicle size classifications used in this work will be introduced next. We worked with two variations that are at the larger end of the scale of the vesicle sizes, called large unilamellar vesicle (LUV, diameter 0.1-1μm) and giant unilamellar vesicles (GUV diameter 100-1μm). Similarities exist between the two classes of vesicles, and in both cases the vesicle diameter is large enough in comparison to the thickness of the bilayer that individual molecular properties may be

ignored and treated collectively as the material property of the membrane. In our experiments we consider a highly organized body made of one material with uniform material properties, able to enclose a volume that separates inside and outside with a closed barrier that is less than 5nm thick. The liposomes here are composed of a fundamental constituent of a cellular membrane, phospholipids. As such they offer a starting point from where the study of membrane physics logically begins. Before taking a step forward we will start by looking at the some of the mechanical properties that characterize phospholipid membranes.

Forces Involved with Membrane Stability

In these aggregates surfactants are extremely stable. They are stabilized by a balance between two factors, aggregate pressure and molecular spacing. The molecular spacing is expressed by the optimal head group area, where as the pressure is a balance between packing of the hydrophobic core and minimization of core's surface area to the hydrophilic interface. These two factors are best described by an interfacial tension. The tension acts to hold the amphiphiles in their specific aggregate and keep the aggregates stable in solution. In fact, it has been determined that the characteristic times that lipids typically reside in a bilayer are on the order of $\tau_R = 10^4$ seconds (Wimley and Thompson 1990)**,** such residence times have a direct impact on the stability of liposomes. The process of lipid escape from a bilayer is dependent on how much energy it takes to put an alkane into a hydrophilic environment. Another process, the exchange of a lipid from one monolayer to another monolayer in a bilayer, called flip-flop, considers the opposite and is dependent on the energy costs associated with movement of a hydrophilic head through a hydrophobic barrier. For such a process residence times have been calculated to be on the order of $\tau_R = 10^5$ seconds (Wimley and Thompson 1990)**.** The result is vesicle membrane stability on the order of months. Of course these are not the only effects involved in liposome stability, but they are primary considerations.

D. Membrane *properties*

Liposome stability also depends on the thermo-mechanical properties of the membrane. Below a certain temperature, T_c, the properties and morphologies of the vesicles change drastically. One is able to determine this transition temperature, T_c, and the factors affecting it fairly effectively using a heat measuring technique like differential scanning calorimetry (DSC). The transition, often referred to as a gel to fluid transition, physically is best described by an increased mobility in the lipid tails as well as an increased mobility of the lipid in a bilayer. Factors such as hydrocarbon chain length and saturation, and different types of lipid in a bilayer have a pronounced effect on the transition temperature. Above the transition temperature the bilayer membrane is considered an isotropic two dimensional fluid where the lipids are free to diffuse laterally. From this reference point we try to understand the physics of membrane fusion through an understanding of the membrane mechanical and statistical mechanical properties and the energies associated with them.

Phospholipid bilayers are reluctant to allow just any molecule to pass across its membrane. In biological systems, proteins aid the transport of larger and charged molecules across the bilayer. In vesicles, for example our simple closed lecithin membranes, there is no such mechanism to facilitate the transport of molecules. In the absence of stresses, such as a gel fluid-phase transition, they are impermeable to most molecules other than water. For comparison permeability coefficients (P) of lecithin bilayers to water are P_{water} $=10^{-3}$ -10^{-4} cm/s, where glucose has a permeability coefficient of $P_{glucose}$ $=10^{-8}$ cm/s, and anion and cations, have an even smaller permeability coefficient, P_{anions} $=10^{-10}$ cm/s. In real terms that means that approximately $3x10^4$ water molecules pass through the bilayer every second, where as it takes on the as much as 70 hours to pass a single sodium ion across a bilayer (Lasic 1993). As such we consider the bilayer impermeable to molecules other to water.

A lipid bilayer which makes up a vesicle membrane can be considered a two-dimensional surface in a three dimensional space. Every point on the membrane surface can be described by two principal curvatures, C_1 and C_2. Taking into account the entire membrane surface one can describe its curvature energy, the energy needed

to deform a segment of membrane area (dA), using the following effective Hamiltonian.

$$E_b = \int \left(\frac{k_b}{2}(C_1 + C_2)^2 + \kappa_g C_1 C_2 \right) dA$$

The expression depends on the mean , $\frac{1}{2}(C_1 + C_2)$, and Gaussian curvatures, ($C_1 C_2$), and the constants that describe the material properties of the membrane, the bending (k_b) and Gaussian curvature (κ_g) moduli. As such the energy associated with a closed membrane surface like that of a vesicle can be described as a sum of the two terms above.

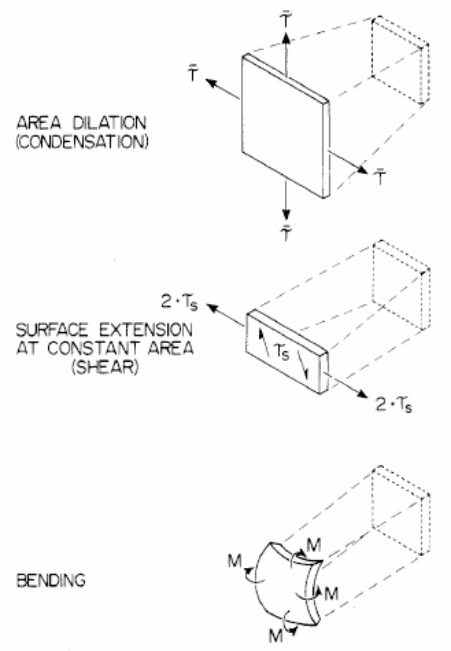

Figure I-6. Membrane Deformations: The figure show three different modes of mechanical deformation associated with lipid membranes; shear, bending, and stretching. Mechanical stretching is energetically more demanding than either shear or bending of the membrane (Evans and Parsegian 1983).

The mechanics of a membrane can be associated with three different deformations; stretching, shear, or bending, as illustrated in Figure I-6. Addressing the mechanics of membranes on the length scale of micrometers, characterization of bilayer depends on the collective properties of the lipids that make up the bilayer, in this way it is sometimes modeled as an infinitely thin elastic sheet (Seifert 1997). The energy of all three deformations are scaled by constants that define the material properties of the membrane, its viscosity, and bending and stretching moduli. For a

number of single component lipid bilayers these material properties have been measured using various experimental techniques (Luisi and Walde 2000).

Working with fluid membranes, the forces need to deform it by bending and shearing are negligible compared with stretching deformations. In this respect shear deformation is not usually considered in a fluid membrane bilayer (Helfrich 1973). Two types of membrane shear exist, intermonolayer shear and shear with respect to lipids in the same monolayer. As long as the two monolayers of the bilayer are not coupled they remain independent and are able to slide over one another without resistance. Inside the bilayer forces are isotropic and the lipids are free to diffuse with little or no in-plane resistance. Lipid bilayers are also able to withstand other stresses such as bending or stretching. The energy scale associated with the bending deformation is governed by the bending modulus and is characterized by a material property called the bending rigidity. For bending there is an increase in the area per molecule in the outer monolayer and a decrease in the area per molecule in the inner monolayer of the bilayer. Similarly the stretching modulus and stretching elasticity describe the stretching deformations associated with a bilayer. Stretching of the membrane results in an identical change in both the inner and outer monolayers.

Using giant unilamellar vesicles as probes it has been shown that one is able to determine such macroscopic membrane material properties. A particularly effective apparatus used to do this is the combination of optical microscopy and microscopic glass capillaries, called micropipettes. Using such an apparatus one can determine membrane viscosity, or bending and stretching moduli with great precision (Evans 1980). Using a glass capillary with a diameter smaller than the vesicle diameter, one is able to apply a suction pressure to the vesicle and induce a tension in the membrane. At low suction pressures one is able to determine values for bending elasticity, (SOPC - 10^{-19} J, EPC 0.4-2.3 10^{-19} J), and at higher suction pressure one is able to determine the area expansion modulus (PC-PE membranes 200-300 mN/m respectively, EPC 140 mN/m) (Needham and Nunn 1990), as well as determine where the membrane eventually fails, called tensile failure or lysis tension. In addition to the above mentioned properties one can also measure changes in the bilayer membrane before and after bilayer phase transitions, this includes bilayer permeability and shear viscosity when the bilayer is in the gel state. These properties differ depending on

bilayers composition (i.e. presence of cholesterol, presence of different lipid, or surfactants) or lipid architecture (Needham and Zhelev 1996). Drawbacks to using such techniques is that collection of data that leads to reliable statistical analysis is very labor intensive, additionally membrane properties have been shown to vary dependent on preparation procedures (Lasic 1993).

Data from measurements on submicroscopic lipid vesicles is determined as a statistical average over a large number of vesicles dispersed in solution. Techniques like ultrasonic velocimetry are used to determine material properties like volume compressibility. As mentioned before structural characteristics like bilayer thickness, vesicle size or aggregation of the small vesicles are determined using various scattering techniques, like neutron and x-ray and light scattering (Van Zanten 1996). Fluorescence studies are used to reveal lateral diffusion properties of lipids in membranes, phase separation in multicomponent lipid bilayers, and mixing of contents between two opposing lipid bilayers or vesicle volumes during membrane fusion (Duportail and Lianos 1996; Pantazatos and MacDonald 1999; Heuvingh, Pincet et al. 2004) .

The complex characteristics, behavior, and intermediate structures involved in the fusion process must depend on the general mechanical and surface properties of the lipid bilayer. In this way we use pure lipid membranes, as such we are able to remove the complexity that plagues the experimental investigation of fusion in purely biological systems, and concentrate on the physical factors that are involved. Liposome interaction and stability can be influenced by changing external parameters such as pressure, which imposes mechanical stresses or strains on the bilayer. We can control the composition of the membrane, and examine the influences due to changes in its composition, and study fusion based on the contributions and interactions of particular inclusions in the membrane. By focusing on the basic physical laws that govern membranes we attempt to break down inter-membrane interactions and determine the general aspects leading up to fusion.

E. Membrane-Membrane Interactions

Some qualities of liposomes like size, shape, membrane properties, and composition allow them to be described as colloids. As such first attempts to describe aggregation behavior of nanosized liposomes employed a successful theory from colloidal science called DLVO (Derjaguin, Landau, Verwey, and Overbeek) theory. Treating water as a continuous medium DLVO theory was able to successfully describe the stability of colloids based on attractive van der Waals (V_{vdW}) and repulsive electrostatic (V_{est}) interactions. One area where it fails to correctly describe colloidal behavior is the aggregation of uncharged soft hydrophilic surfaces like small or large unilamellar vesicles. Therefore additional contributions (V_{add}) were considered, and applied, to explain the lack of aggregation between bilayer membranes.

$$V_{DLVO} = -V_{vdW} + V_{est} + V_{add}$$

The Van der Waals potential is a strictly attractive potential. For planar surfaces the potential is expressed as

$$V_{vdW} = -\frac{A}{12\pi D^2}$$

where A is the Hammacker constant, and D is the distance between two surfaces. In absence of electrostatic interactions Van der Waals forces can have an effect over a range of up to 15 nm, in which case they should act to induce the adhesion of colloids, planar surfaces, or large or small vesicles.

The electrostatic colloidal interactions are described as a function of the surface charge density, the Debye length, and the distance between two surfaces. Once surfaces become charged, especially having surfaces with identical surface charge densities, they repel one another. The electrostatic potential (V_{est}) between two (like) charged colloidal particles is always repulsive.

$$V_{est} = \frac{2\sigma^2}{\kappa\varepsilon\varepsilon_o} e^{-\kappa D}$$

Where the surface charge density is expressed as σ, the depth of electric double layer by the Debye length κ^{-1}, and the distance between the two surfaces D, The other terms, the permittivity of free space ε_o, and the dielectric constant of the solution ε (for H_20 = 78.5) are constants in a particular system. As shown in the last equation, the potential energy between two planar surfaces can be expressed as a function of two primary factors, the surface charge density, and their separation distance.

The depth of this electric double layer described mathematically by Debye,

$$\kappa = \sum_i \left(\rho_\infty \mathrm{e}^2 z_i^2 \Big/ \varepsilon\varepsilon_o \mathrm{kT} \right)^{\frac{1}{2}} m^{-1}$$

Whatever the charged surface is there is always a collection of oppositely charged counterions in a layer that exists in thermal motion close to the surface, called the electric double layer. In the equation for the electrostatic potential, κ^{-1} describes how electrostatic repulsion between two charged surfaces changes as a result of ionic strength. It is a consideration when electrolytes are present in the solution and depends on the properties of the solution (i.e. concentration ρ_∞ and ionic charge z) and not on the properties of the colloidal surface, like its charge density or surface potential. One is able to reduce the repulsion of charged surfaces by increasing the concentration of electrolyte in solution. By adjusting the ionic strength one is able to adjust the interaction potential between colloidal particles and affect either their aggregation or stability.

Reasons that application of the DLVO theory eludes a successful description of aggregation behavior of uncharged surfaces of liposomes is that it does not include molecular details or the elasticity of the lipid bilayer. The former contribution only takes place over short distances, on molecular scales, the latter has infinite range. Molecular details are described by such properties as surface roughness and hydration layers. The elasticity of the bilayer is displayed in its extreme softness. This can be observed optically under the microscope by thermally driven fluctuations in flaccid vesicles. Both of these interactions act to keep liposomes separated.

On molecular length scales stability of liposomes can be traced to two separate physical forces, hydration forces and a second that is collectively called steric forces. Hydration forces dominate at small separations and arise whenever molecules are associated with hydrophilic surfaces, such as the head groups of lipid molecules. Although the molecules are in constant exchange at the interface measurements using force balance techniques show that forces due to their presence exist and act to strongly repel surfaces over a range from 1-3 nm (Marra and Israelachvili 1985). When bilayers are brought together the water molecules in the hydration layer act to keep them apart. The depth of the hydration layer has been experimentally demonstrated to represent a spatial barrier to membrane adhesion that is approximately 1 nm for each surface (Rand and Parsegian 1989). Also acting on molecular length scales one can attribute a surface roughness to a lipid bilayer. This is due to the thermal fluctuations of individual lipid molecules in the direction normal to the bilayer surface. In this way they are sometimes referred to as molecular protrusions (fluctuations), or steric forces. Due to the similarity between length scales it is difficult to disentangle the contributions from each effect experimentally, but it has been shown that they are both repulsive and together are regarded as V_{mol} in the equation below.

Undulation forces, sometimes also referred to as steric forces, are dependent on the lateral dimensions of the bilayer, but have the potential to act on longer length scales than even electrostatic forces. In a flaccid, tensionless, membrane the undulations are a product of the extreme softness of phospholipid bilayers, described by the bending elastic modulus, k_b, a material property. It describes how hard it is to bend a membrane, the energy needed to bend a membrane which is on the order of 10^{-19} J for PC membranes. That is approximately the equivalent of several kT, and thus the molecular motion of water is enough to induce fluctuations in a membrane. The range of these repulsive forces is completely dependent on the size of the vesicle. Fluctuations in giant vesicles can be observed optically with the aid of a microscope. Considering magnitude, the forces per unit area of the fluctuations are a function of distance D, temperature T, and the bending modulus k_b, as given in the expression below .

$$F_{und} \approx \frac{(kT)^2}{2k_b D^3}$$

This expression when applied to lipid bilayers in the presence of an opposing surface, is sometimes referred to as an entropic pressure.

The combination of the hydration and undulation forces have been proposed to describe the stability attributed to small and large vesicles in solution. Re-written in terms of an interaction potential one has a complete expression to describe the interaction between membranes and lipid vesicles.

$$V = -V_{vdW} + V_{est} + V_{mol} + V_{und}$$

Although the equation above describes the factors contributing to the potential between two soft lipid bilayers, it doesn't describe the magnitudes of the components. Experimentally some of the contributions can be scaled. With the exception of Van der Waals interactions and surface roughness, one is able to adjust the magnitude of hydration layers, membrane fluctuations, and electrostatic interactions. The electrostatic potential is scaled by addition of electrolytes. To a degree one is also able to reduce the repulsive forces due to undulations and hydration layers. To address fluctuations we can apply a mechanical surface tension by aspirating a membrane into a micropipette. Similarly one is able to create an osmotic gradient by placing a vesicle in a hypotonic solution causing it to swell. To address the hydration layers something must absorb the water in the hydration layer. It has been shown that hydrophilic polymers are able to adsorb water from hydration layers to induce adhesion or fusion (Lee and Lentz 1997). Once these factors are addressed, one can determine the effects of specific interaction such as receptor mediated adhesion and fusion.

Ligand-Receptor interactions

Finally in a departure from long range and nonspecific interactions one can begin to discuss the idea of molecular recognition as a way to induce interaction between membranes. The idea of the lock-and-key mechanism introduced by Fisher at

the end of the 19th century was used as an analogy to describe specificity of enzyme action. More recently it was applied to various molecular recognition phenomena and used to describe the process of building supramolecular structures. In general it describes the process of molecular recognition in the absence of the covalent bond formation. Fisher's image was the idea of a steric fit on a molecular level, the synergy between the lock and the key, used to activate a process. Now, the concepts governing the idea of a lock and key mechanism i.e. noncovalent molecular interaction, are being applied not only to biological processes but also to chemical and physical processes as well. Indeed when engineered to do so, ligand and receptor interaction has the potential to play a role in the interaction of membranes and surfaces.

The interaction energies and the strengths of the noncovalent bonds are of interest in the area of biophysics. One particularly well studied model is the molecular linkage between biotin and avidin where binding energies have been measured to be as strong as 35 kT/mole. Due to the specificity of the ligand and receptor interaction the time scale over which binding of many molecules takes place is very slow. When inserted into opposing membranes and the interaction energy is studied, the diffusion of receptors into an adhesion zone ends up being a rate determining step (Needham and Zhelev 1996). The equation below describes the rate of change of binding, $\frac{dN}{dt}$, as a function of the concentration difference in- and outside a contact area, $(C_{in} - C_{out})$, and the diffusion coefficient, D, of the ligand and receptor in the plane of the bilayer.

$$\frac{dN}{dt} = D(C_{in} - C_{out})$$

Intuitively, the interaction of the membranes can be traced back to the number of ligand receptor pairs formed between two membranes. On the other hand the size of the adhesion zone turns out to be a balance between membrane bending and tension and the accumulation of receptors in the contact zone. Another way to put it is that the extent of one vesicle spreading onto another depends on thermodynamic and mechanical considerations. This can be expressed as an adhesion energy, w_a, equal to

the number density of ligand-receptor bonds formed in a given area, (N/A), compared with the thermal energy kT

$$w_a = \frac{N}{A} kT \, .$$

Summary and Objectives

The goal of this work is to address the interactions just described in order to understand interaction in a model system which will lead to membrane fusion. In cooperation with a group from College de France we have engineered a system with which to study model membrane fusion in functionalized vesicles. By incorporating amphiphilic receptors into a lipid bilayer membrane we provide our vesicles with a functional membrane. Doing so we turn the vesicle into a object that is able to differentiate, cooperate, and selectively react with other functionalized vesicles. Necessarily, we must overcome the forces which act to stabilize the vesicle membrane in solution. To do this we employ water-soluble multivalent cations to mediate interaction between different vesicle membranes. Furthermore we utilize specific ligand-receptor interactions to induce changes in membrane properties which will ultimately lead to vesicle fusion.

In a system such as the one described above; consisting of a bilayer membrane, amphiphilic receptors, and ligating component in the form of multivalent cations, one has the components to simulate the actions that govern secretory fusion in biological systems, in a completely artificial environment. In particular, one can envisage reproducing the primary coordination steps exhibited by the general class of SNARE proteins (Figure I-2, pg. 8), where interactions between two types of membrane bound proteins are mediated by a third protein which is free in the extracellular matrix. As such we have the makings of a biomimetic system that has the potential to coordinate the interaction between two vesicles that will lead to membrane fusion and simulate the role of SNARE proteins in a protein free system. The details of the materials used to construct this biomimetic system and means

which we use to induce and characterize these interactions will be described in the following section.

II. Material & Methods

A. Materials

As a goal to induce fusion and study its pathway from a physical perspective, we aim to keep the system extremely simple. In this way we limit the components in our experimental system to only four parts consisting of lipids, receptors, ions, and sugars all in an aqueous environment. What we are left with is a model system which is fairly clean and chemically simple with only essential components which we expect to lead to membrane fusion. As such we have removed the complexity found in biological systems to be able to focus on the essential aspects governing the process of membrane fusion.

1. Lipid

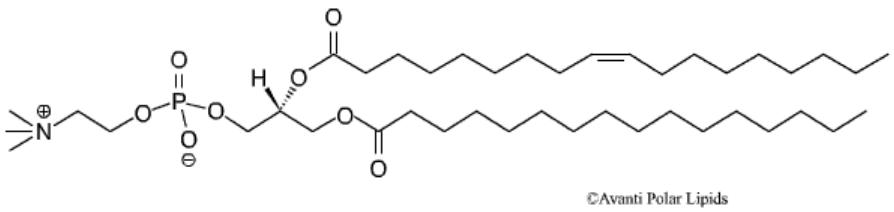

Figure II-1. Lecithin: The chemical structure of a L-α-Lecithin molecule used in the experiments. The head group is identical in all lecithins, but there is variation with respect to the length and number of double bonds in the fatty acid tails that yields an average molecular weight 768 g/mole (Avanti Polar Lipids Webpage).

We build model membranes from a mixture known as known L-α-Phosphatidylcholine (Sigma-Aldrich, Germany), also known as L-α-Lecithin or simply Egg PC (EPC). The lipid is a mixture of phospholipids with identical Phosphatidylcholine head groups (Figure II-2.) and chains that vary in length and saturation. Analysis of the lipid mixture reveals that the fatty acid tails are primarily composed of hydrocarbon chains containing saturated and mono- and di-unsaturated chains (the main components are listed as mole percent, chain length:number of double bonds (chemical name); 33%, C16:0(palmitic), 13% C18:0(stearic), 31% C18:1(oleic), and 15% C18:2 (linoleic)). the molecular weight of the mixture is averaged and found to be 768 g/mol. We produced both giant and small unilamellar vesicles and take advantage of a lipid membrane's ability to solubilize both proteins and other non-lipid amphiphilic molecules. In this way the vesicles act as carriers for

our amphiphilic receptors and we use them as probes to study the physical aspects leading up to fusion.

2. Active solutions

Phospholipid bilayers are semi-permeable membranes. In the absence of stresses, such as a gel fluid-phase transition, they are impermeable to most molecules other than water. In our experiments we use concentration gradients to deflate vesicles to be able to investigate them in a tensionless state. By preparing vesicles, the observation environment, using different concentrations of sucrose or glucose that are lower inside (0.200 Osm) a vesicle than outside (0.205 Osm), one creates an osmotic gradient driving water out of the vesicle. This is equivalent to partially deflating a balloon. This reduces the volume and creates an excess area with respect to the volume to area ratio, where a volume to area ratio equal to one indicates a perfect sphere. Deflating a vesicle using such a concentration gradient, one is able to create zero tension within a vesicle membrane. Such conditions allow us to investigate the interactions of the outside of the vesicle membrane with ions of particular interest.

Many studies have been performed to investigate the interaction between ions, lipids biomembranes (Papahadjopoulos, Vail et al. 1977; Duzgunes, Wilschut et al. 1983). It has been definitively shown that not only do ions change the properties of lipids (Papahadjopoulos, Poste et al. 1973), but they also adsorb, affect the permeability, as well as the stability of bilayers (Altenbach and Seelig 1984; Evans and Metcalfe 1984; Lasic 1993; Lehrman and Seelig 1994). In addition they have been used to induce adhesion between vesicles. In ionic solutions it is generly thought that the effect of chloride ions is negligible, as such we only consider the properties of the cations. Here we use three different cations; Eu(III), Cu(II), Ni(II) to mediate interaction between vesicles. The reason that they have been chosen here is three fold; first, due to their solubility in aqueous solution, in addition their photophysical properties, such as their ability to absorb and emit light at particular wavelengths, and finally, due to their size and electron configuration they are able to coordinate multiple ligands at once.

3. Receptors

Intermembrane recognition is necessary to induce fusion of membranes. In order to coordinate two opposing membranes to induce molecular interactions on the basis of specific molecular recognition we incorporate the molecules shown below into the bilayer membrane. In this respect choice of ligand and receptors is based on the functional moieties that are proven to form molecular complexes with both lanthanide and transition metals (ligands). Interaction between the functional moieties of the two amphiphilic molecules in Figure II-2 and various transition metals is the focus of many coordination chemistry studies reviewed in (Lehn, Sabbatini et al. 1993). Interest in the molecular complexes surrounds their special photophysical properties i.e. absorption, luminescence, and energy transfer, as a result of metal-ligand complex formation. This is in addition to their possible application in metal-ligand fluorescence assay.

Here we use them to promote irreversible binding between a pair of vesicles. The synthesis of amphiphilic receptors used in this work is described elsewhere (Marchi-Artzner, Brienne et al. 2004). The end product of the synthesis is an amphiphilic molecule with two lipophilic anchors in the form of C16 chains, and a two short hydrophilic PEG (4-6) spacers which when fully stretched have a length of 1.5nm. The functional moieties, ß-diketone and bipyridine, form a molecular bridge between amphiphilic chains. Inside the bilayer, both the hydrophilic spacers, fully extended, have a length of ≈ 1.5 nm that act to keep the functional groups exposed in an aqueous environment. The hydrocarbon chains are equivalent in constitution to the 33% (16:0, palmitic) of the tails found in Egg PC lipid mixture. On paper the two

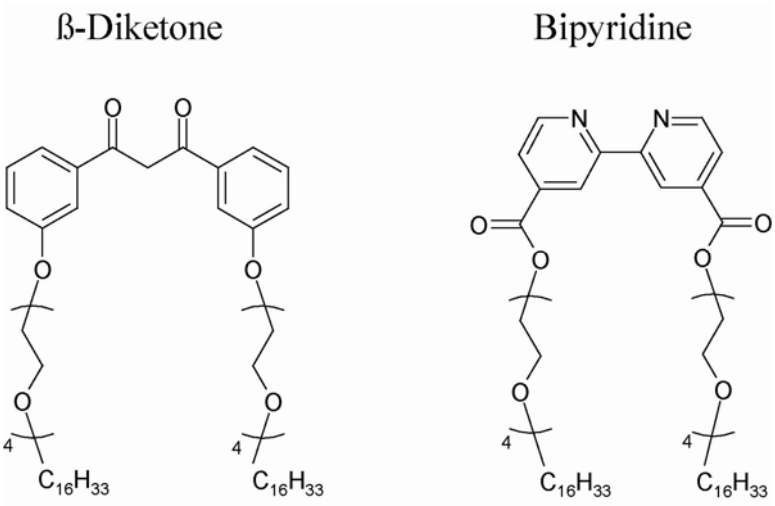

Figure II-2. **Receptors: In appearance there is little difference between the two ligands shown here other than the different functional moieties that are found at the "top" of the two amphiphilic molecules. The molecule called ß-diketone has an average molecular weight of 1057.52 g/mol, and the molecule called bipyridine has an average molecule weight of 1044.61 g/mol**

different amphiphilic receptors, bipyridine and β-diketone, resemble two chained lipid and should incorporate easily into a phospholipid bilayer.

We use the zwitterionic Egg PC lipid (EPC) to form neutral membrane surfaces, our vesicle probes. All observations were carried out in aqueous sugar solutions. We use pure Egg PC membranes as a reference probe. When functionalized, the lipid bilayer membranes act as carriers for the ligand. We can adjust the constituents of our fusion probe depending on the lipid to ligand ratio, and we can achieve our goal of investigating the role of ligand in vesicle fusion by mediating the interaction of the membranes using the appropriate ion. With only three to four active components in our system we will try to disentangle the ion-membrane and ion-ligand interactions uncover the physical aspects governing, or leading up to fusion between lipid membranes.

B. Vesicle Preparation

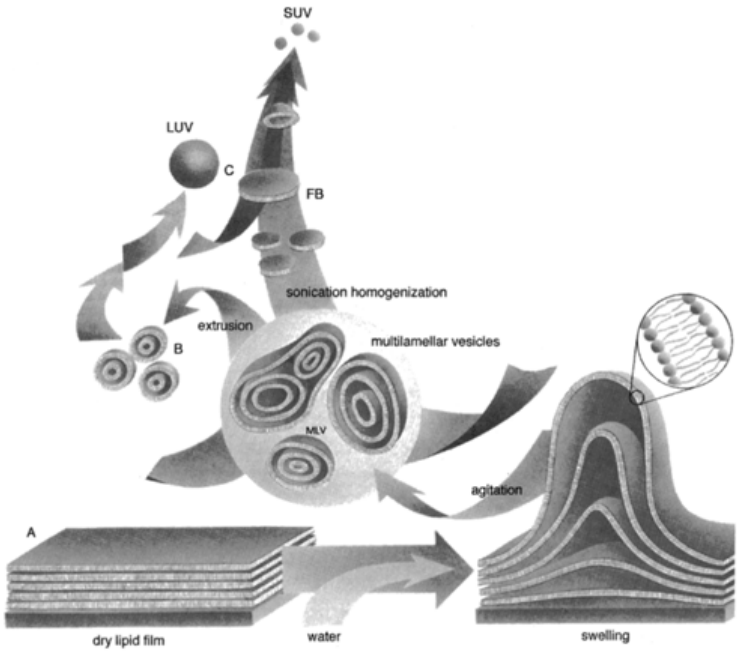

Figure II-3 Evolution of Vesicles: The figure shows how one arrives at different classes of vesicles beginning from a stack of lipid bilayers. Practicing a protocol of hydration followed by agitation one is able to build a wide variety liposomes depending on experimental needs (Avanti Polar Lipids).

All phospholipids are insoluble in water and simple mixing of lipid and water doesn't result in spontaneous small or giant unilamellar vesicle formation. In the late sixties Reeves and Dowben investigated the effects of swelling thin lipid films in aqueous solutions, and developed a protocol for making giant vesicles (Reeves and Dowben 1968). Since then variations on vesicle formation have been developed and many different preparation methods currently exist. One must predetermine the type of liposome needed for a measurement taking into account factors such as size, composition, and membrane sensitivity. Here we describe the two protocols used to construct vesicles in this work, one for production of giant unilamellar vesicles GUV's (diameter >10 μm) and the other for large unilamellar vesicles LUV's (diameter > 0.1 μm).

There are a few features that are common to both giant unilamellar vesicle and large unilamellar preparation techniques. The initial step to creating vesicles here is to create a lipid film. One does this by depositing a volume of lipid solubilized in an organic solvent; usually chloroform, into a container (in the case of extrusion of LUV's), or onto conductive surface (in the case of electroformation GUV (details of

the deposition will be given below). In both cases, based on the amount of lipid deposited and the type of container that it is deposited into, one dries the prepared lipid solution under vacuum until dry. Finally, vesicle formation takes place with the addition of aqueous solution to the lipid film. In order to obtain vesicles with different size one must now vary the preparation procedures significantly.

1. Extrusion

One is able to produce uniform submicron sized unilamellar vesicles using a technique called extrusion. It is the method of choice for producing well defined, small and large unilamellar vesicles (Lasic, Liposomes). Here high pressure is used to force a dispersion of multilamellar vesicles through pores with a well-defined pores size. Repeated cycling of the vesicle dispersion through the filters reduces the number of lamellae per vesicle. In the end the extrusion process gives expected results, unilamellar lipid bilayers with a narrow distribution of vesicle sizes having a mean diameter near the filter's pore size.

Extrusion of vesicles

- Starting from a stock solution of lecithin in chloroform 100mM (76.1 mg/ml)
- 2ml placed in a 5ml flask and diluted to 31.45 mM
- Placed in a desiccator overnight
- Addition of 2.2 ml of glucose 200mM
- Closed and placed in the oven (50 C)
- Vigorously shaken for 45 – 60 minutes (1000rpm), until film completely mixed
- 2.2ml of the lipid dispersion placed in the extruder (Lipofast Pneumatic; Avestin Inc, Canada)

All nanopore filters, Nucleopore Etchtrack; Whatmann Int., UK

- Extruded through filter, 400nm pore size 31 times
- Extruded through filter, 200nm pore size 31 times
- Extruded through filter, 100nm pore size 61 times
- The solution is removed from the extruder and diluted with 200 mM glucose solution to a concentration of 10 mM.

2. Electroformation

Giant vesicles are ideal objects to model cell bodies, particularly with respect to size and composition. In our case we take advantage of the size of the giant vesicle in order to visualize, and physically manipulate the vesicles using optical microscopy and micropipettes (described below). One proven method to produce unilamellar giant vesicles is using a technique called electroformation. Two parallel conductive surfaces, here indium tin oxide (ITO) glass plates, and a non conductive dielectric spacer that separates the two ITO plates form a liposome electroformation chamber. 2 μl of 2mg/ml EPC chloroform solution is spread on the ITO glass to create a thin lipid film. This film is placed in a desiccator for at least two hours to remove any traces of chloroform from the lipid film. After this period, the electroformation chamber is assembled. One side of the 2mm thick dielectric frame is lined with high viscosity silicon grease. The spacer is then placed on the conductive side of the ITO glass. The chamber is completed by lining the opposite side of the dielectric frame with the same silicon grease, and placing the second piece of ITO glass with the thin lipid film on top of the frame. This yields a closed chamber with the two pieces of ITO glass, conductive sides facing one another, separated by a 2 mm thick dielectric frame. Two electrodes connected to a function generator are attached to the conductive sides of the ITO plates. The chamber is filled through one of two, 1mm diameter, fill ports located in the side of the dielectric frame.

The electroformation chamber holds approximately 2ml of the desired solution. In our case the giant vesicles prepared were in a 200 mM solution of glucose. After electroformation, one is able to control factors such as membrane tension, vesicle volume, and depth in solution and enhance optical contrast using the appropriate solution. Once the electroformation chamber is filled, 10 Hz, low voltage AC field is applied to the system to induce separation of the thin lipid film from the substrate. The voltage and duration of the applied field used in this work are given below.

The electroformation process is concluded by slowly decreasing the AC frequency to 0.5 Hz and leaving it for 1 minute before turning off the function generator. The reduced frequency facilitates removal of the individual vesicles from the substrate and electroformation chamber after they have been formed. The chamber is opened by removing the ITO plate that doesn't have the lipid applied to it. Using a

modified 1ml (1000μl) eppendorf pipette tip with a larger opening, 0.750 ml of the solution is aspirated and placed into a 2.0 ml sealable test tube. The aspiration process is repeated until the entire solution is collected. Generally electroformed vesicles have diameters that range from 5-200μm in diameter. Ideally, one is interested in only unilamellar vesicles, more than one bilayer will cause problems with respect to its mechanical properties and our ability to induce fusion. As such they are the ideal model objects for performing micromanipulation and local microinjection experiments.

Electroformation of vesicles

- 2.6mM (2mg/ml)
- 2µl spread in a thin film on an 5cm^2 ITO plate
- Placed in a desiccator for ~ 120 minutes
- Addition of ~ 2 ml of sucrose 200mM into electroformation chamber
- Electroformation chamber connected to a function generator, and a low frequency AC electric field turned on:

Applied field:

- 10 Hz, 1.0 V_{pp} 30 minutes
- 10 Hz, 1.5 V_{pp} 30 minutes
- 10 Hz, 2.0 V_{pp} 30 minutes
- 10 Hz, 2.5 V_{pp} 30-120 minutes

C. Analytical Methods

To investigate the physical aspects of fusion we choose to use a series of complementary experimental techniques to determine the changes in the free energy of the system. To investigate the interaction of ions with membranes or ligands we perform isothermal titration calorimetry (ITC) measurements. Using ITC one can determine thermodynamic quantities such as molar enthalpy, entropy, or free energy. Dynamic light scattering measurements complement the ITC measurements and are used to determine changes in vesicle radius and size distribution of vesicles. Changes in vesicle size can be correlated with adhesion or fusion of vesicles. The two techniques are performed on large unilamellar vesicles, which are invisible to the microscope. Thus direct visualization of the submicroscopic processes measured using ITC and DLS is performed on giant vesicles by optical microscopy. One can employ advanced light microscopy for direct visualization of membrane-membrane interaction. In combination with light microscopy micropipettes are used to

manipulate, induce forces and measure interfacial free energy due to intermembrane interaction. Comparison of the results from the nanoscopic (ITC & DLS) and microscopic systems should allow us to build a complete picture of the energy and processes leading up to and involved in the process of fusion.

1. Isothermal Titration Calorimetry

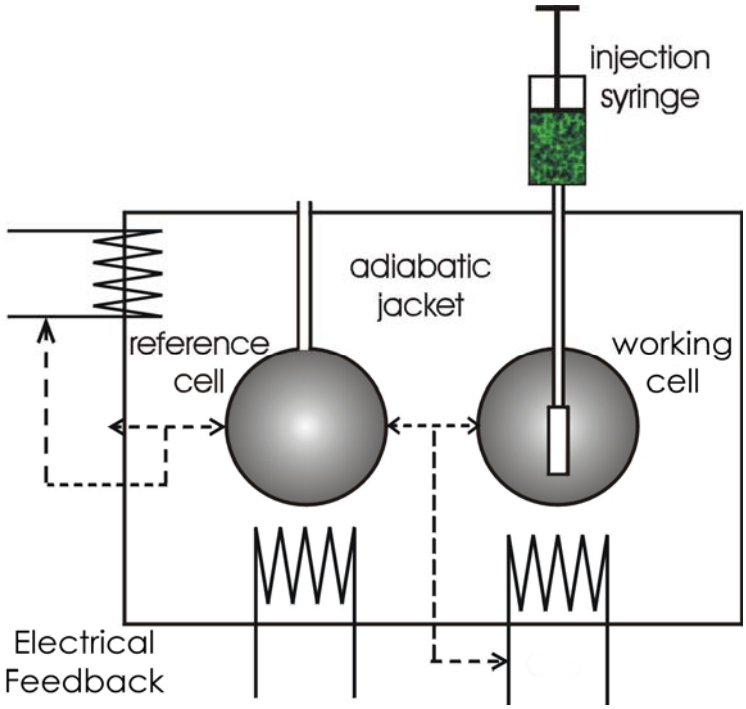

Figure II-4. Isothermal Titration Calorimeter: A schematic diagram of the isothermal titration calorimeter. Both the working and reference cells hold a volume of 1.442 ml. The injection syringe is capable of injecting up to 0.300 ml. The temperature is maintained via a differential electrical feedback system that works to keep both working and reference cells at a constant temperature. In addition a separate feedback system maintains an equilibrium temperature between the reference cell and the external environment. In this way one has an apparatus operating in an isothermal, adiabatic environment.

One particular advantage of ITC is that it allows measurement of interactions in their native state without need for molecular labeling. Almost all chemical and physical processes entail changes in heat, and thus can be measured with ITC. There are two different cell volumes (both 1.44 ml), a working cell and a reference cell (Figure II-4.), housed in an adiabatic (no heat exchange) jacket. The contents of two solutions are mixed in the working cell using precise injections (± 0.1 μl) through a motorized injection syringe (volume 0.3 ml). Temperature differences between the two cells are measured, the differential power needed to equilibrate the two cells is input and used to maintain temperature equilibrium. The raw signal has units of

power, and integration of the signal with respect to time yields a measurement of thermal energy. In this way using the ITC one measures the heat evolved in a reaction which is released proportional to the amount, or number of moles, of binding that occurs.

An ITC experiment directly measures the heat absorbed or evolved in liquid samples as a result of mixing precise amounts of two solutions. ITC is one of few direct methods, along with other calorimetric techniques, for determining the molar enthalpy change (ΔH) of a reaction. It is the most direct method to measure the heat change based on complex formation at constant temperature. The apparatus is extremely sensitive and can measure the change in temperature within a μK in a cell with a volume of 1 ml and has a noise of 0.1 ncal/sec associated with the measurement signal. This allows very precise characterization of energies involved in formation of bimolecular complexes. With such sensitivity one is able to determine binding affinity with a great degree of accuracy.

A quantitative description of forces and energies that govern the formation of ligand-receptor complexes is part of this endeavor. Several models exist that are used to describe the adsorption of molecules to surfaces and ligand-receptor interactions. In equilibrium the ratio of the amount of free molecules vs. the amount of bound molecules is defined by the equilibrium constant. The models used to describe adsorption are usually based on equivalent and independent binding sites. At constant temperature variation of bound molecules to a surface is called an isotherm. Using physically plausible assumptions the most frequently used isotherm is the Langmuir isotherm. The models that we apply to our data will be addressed in the discussion of the ITC results.

In our case the experiment was designed such that the initial injection from the syringe, the ligands, into the working cell, the receptor, results in the binding of all of the added ligand. This generates the maximum heat associated with the system. The heat of binding is a result of the interaction of the ions with receptors on the outer surface of the membrane in functionalized vesicles and the lipid molecules in unfunctionalized, pure Egg PC vesicles. Binding affinity is determined from fitting of the measured data and using the equilibrium constants as a fitting parameter. Finally it

should be possible to derive the complete thermodynamic picture with respect to enthalpy (ΔH), entropy (ΔS), and Gibbs free energy (ΔG) with respect to the ion-membrane and ligand (cation)-receptor interaction.

At constant pressure changes in energy for a given system are directly related to the changes in enthalpy in an adiabatic environment and are expressed with the equation below

$$\Delta G = \Delta H - T\Delta S$$

Using this relationship we should be able to develop the complete thermodynamic picture with respect to ligand-receptor interaction from the changes in heat flow measured throughout a given measurement. The next equation describes how the measured changes in enthalpy (Δh) are related to the molar enthalpy (ΔH) and the fraction of ligand bound to the receptor, or adsorbed on a surface (X_b).

$$\Delta h \propto \Delta H\, X_b$$

In addition using the appropriate adsorption model (described in the results section when they are applied to the experimental data) one is able to describe the fraction of ligand bound to the receptor in terms of other thermodynamic quantities, in particular the equilibrium constant (K), which describes the affinity of the ions for the membrane or a particular receptor.

$$\Delta G = -RT \ln K$$

After determining the above mentioned quantities one is able to develop a complete thermodynamic picture with respect to enthalpy, entropy, and free energy of the system.

The difficulty with the analysis of the measured data lies in the fact that the observed heat change, which is the immediate outcome, is a global property. Free energy of complex formation turns out to be a small number resulting from a delicate

balance between favorable and unfavorable contributions. Moreover binding takes place only if the total free energy change decreases, regardless of the actual amount of favorable free energy change accumulated by direct molecular contact between associating molecules. That is to say solvent effects are as important to the energy balance as the direct noncovalent interactions. However careful reference measurements should eliminate some of this interference, and help distinguish between ion-membrane, ligand (cation)-receptor interactions and inter-membrane.

Isothermal titration calorimeter (VPITC Microcal, UK) was used to determine the binding constant as a result of the interaction of different electrolyte solutions with large unilamellar lecithin vesicles and functionalized large unilamellar lecithin vesicles. The total lipid concentration in each experiment was 10 mM and the average vesicle diameter was always close to 100nm. 10µl aliquots of a low concentration (1,2, or 5 mM) osmotically balanced, electrolyte solution, either $EuCl_3$, $GdCl_3$, $NiCl_3$, $CuCl_3$, was injected into a large unilamellar vesicle suspension at 25^o C. Each injection was performed over a period of 4 seconds. The heat flow was measured for up to 240 seconds before the subsequent injection took place. After the experiment was performed, the heat flow could be plotted as a function of time and changes in heat as result of the injection volumes could be analyzed. Following the measurement the vesicle dispersion was prepared for light scattering characterization.

2. Light Scattering

Dynamic light scattering, another non invasive analytical method, is particularly useful for samples containing homogenous particle size and shape. One is able to determine information about the size and size distribution of vesicles from a sample measurement. The hydrodynamic radius is determined as a function of the diffusion coefficient, which in turn is determined from the correlation from intensity fluctuations in scattering intensity. As such, light scattering allows us to maintain the integrity of the system without the addition of impurities of dyes, or adding markers to our sample. Here we use dynamic light scattering to compliment the measurements performed by isothermal titration calorimetry.

Using light scattering apparatus (ALV-NIBS; ALV, Germany) one can determine the hydrodynamic radius and polydispersity of particles, in our case radius of large unilamellar vesicles. This makes its characterization of vesicle dispersions particularly useful when studying vesicle aggregation and fusion. We perform two measurements. One before the ITC measurement (no electrolyte) and compare this with a measurement made after the ITC experiment (electrolyte). Comparisons of the two measurements, before and after the ITC experiment, give us information about changes in the size distribution of the vesicles as a result of the interaction of the membranes with the electrolyte.

Non invasive back light scattering was used to determine vesicle size distribution as a result of a given extrusion procedure. Samples were illuminated with a He-Ne laser emitting a wavelength of 632.8 nm and colleted at a back scattering angle of 173^{o}. 1.5-2.0 ml of vesicle dispersion (10mM lecithin concentration) was placed in a disposable cuvette and degassed for 5 minutes at 24 C. The scattered light intensity was averaged for 3 minutes and measured at 25° C.

3. Microscopy and Image Analysis

Experiments on giant vesicles were performed using optical microscopy, the preferred experimental technique used in this work. Direct visualization, in real time, of what takes place as a result of the injection of a particular electrolyte allows us to see the difference between ion-vesicle and vesicle-vesicle interactions. In addition optical microscopy with digital video processing can image fast, very thin optical sections, advancing its spatial limits to the nanometer regime and its temporal limits to the microsecond regime. In particular two advanced microscopic techniques, differential interference contrast (DIC) and phase contrast microscopy, have been employed here to aid visualization of the vesicles under the microscope, without the addition of stains or dies in our samples.

Fritz Zernike (Phase Contrast) and Georges Nomarski (DIC) have advanced microscopy by using the principles of light and optics to enhance interference or contrast in objects that would not normally be seen, allowing visualization of the

invisible. Both techniques use optical components to enhance contrast and or create interference when light passes through a specimen. Phase contrast takes advantage of a phase shift in the transmitted light after it passes through a sample. Using optical components one is able to ensure that the phase difference between deviated and undeviated light is $\lambda/2$ out of phase when it is recombined in the optical plane. Differential interference contrast microscopy alters the ray path of light according to varying sample thickness and refractive index to give the sample a pseudo three dimensional appearance. Here intensity differences are related to the rate of change of the refractive index and specimen thickness, resulting in an exaggeration of its optical thickness (Figure II-9) .

Two other microscopic methods were used to compliment interactions studied using phase contrast microscopy. Reflection interference contrast (RICM) and fluorescence microscopies were used to observe interactions between the vesicle membrane and glass surface, and ligand-receptor complex formation, respectively. Both techniques use incident-light Hg lamp as an illumination source. RICM maximizes interference due to reflected light from surfaces at the glass-water and water-membrane interface. Doing so allows one to estimate the proximity of the membrane to the surface and monitor membrane spreading as a result of adhesion to glass or rupture of the lipid bilayer. Use of the Hg lamp also allowed for application of fluorescence microscopy in the study of ligand-receptor complex formation.

As such using these four methods of optical microscopy, we should be able to accurately characterize membrane interactions by using:

- RICM to observe the interaction between the membrane and the glass surface.
- DIC to accurately observe macroscopic membrane-membrane interactions
- Fluorescent microscopy to determine the formation of ligand-receptor complexes.
- phase contrast microscopy to monitor the exchange of contents between two vesicles, or vesicles and the surrounding solution.

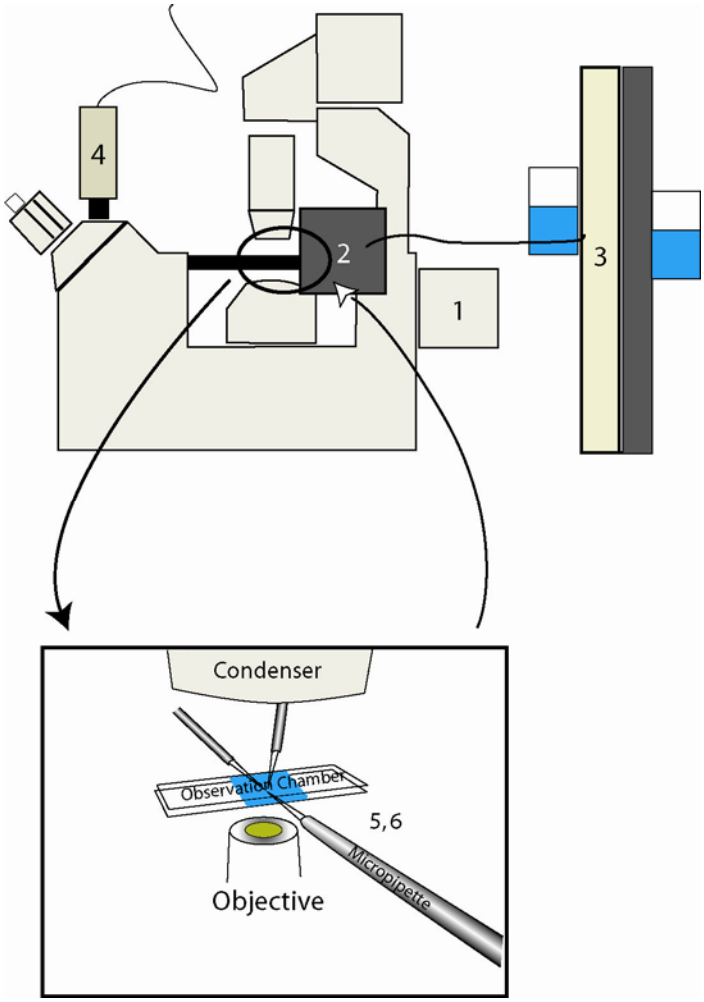

Figure II-3. Micro-manipulators & –scope: The figure above shows the microscope and micropipette set up. The microscope has a Hg Lamp for fluorescence illumination (1) and equipped with a digital camera (4) to facilitate data acquisition. In addition the microscope has been modified to accommodate up to three micropositioners (2). The observation chamber (5) can hold up to 1 ml of solution and handle up to three micropipettes (6). Pressure in the micropipettes is controlled via hydrostatic pressure differences using water reservoirs mounted on a linear translation stage (3).

4. Optical microscopy

The experimental set up used to perform measurements on giant vesicles is centered around an inverted light microscope (Axiovert 135 TV; Zeiss, Germany) that is suited for phase contrast, differential interference contrast (DIC), epifluorescence and bright field microscopies and reflection interference contrast (RICM). To induce and quantify the interactions between vesicles and finally archive them, we modified the microscope with up to three micromanipulators (Sutter Instruments, USA; Narishige, Japan), a digital camera, and video recorder. Observations were made using either a 20x, NA 0.5 or 40x, NA 0.75 phase contrast objectives (Zeiss,

Germany) and recorded using digital cameras with CCD or CMOS sensors. Optical microscopy was used to detect interactions such as adhesion and fusion between vesicles as a result of local injections of electrolyte solutions using a micropipette in the vicinity of a group or pair of vesicles.

Archiving and recording the results of measurements has been facilitated by the two cameras attached to the microscope and in particular, a high speed camera. However the description of the application of the basic CCD camera is discussed first. A black and white KP-M1ZEK CCD camera (Hitachi, Japan), with a sensor that is 768 x 493 pixels (imaging size (8.8 x 6.6 mm)), is mounted below the microscope and is connected to a video recorder and computer. Both signals are then displayed on separately and continuously monitored. As such one is able to simultaneously record experiments, and capture images online while the experiment is being performed. The CCD camera is useful for continuous recording of long-time experiments, where results and observations are made on the order of 10 minutes or longer. Images can be captured in real time or from video tape after the experiment has been performed.

The second camera (Redlake HGK 4000, USA) is mounted above the oculars on the microscope and slightly more sophisticated. It is a high-speed camera that records images at up to 100,000 frames per second (fps). The recorded images are stored on a hard disk directly built into the camera itself. The camera uses a 1504x1128 pixel CMOS sensor feeds the live video to a computer and onto a monitor, while simultaneously recording in a cycle discarding information that is not used. The time that the video is recorded is dependent on the size of the image, and frame rate that one uses (faster frame rates result in shorter recording times). At frame rates that we use, 30-30,000 fps, the recording time is on the order of 400 to 5 seconds, respectively. Once the sequence recording cycle is stopped it can be downloaded from the hard drive on the camera to a computer hard drive and subsequently analyzed. Currently the factors limiting the temporal resolution of the camera are the strength of the light source, and the recording of an image with enough spatial area that will reveal the information about the process of fusion. Using a mercury lamp we are able to achieve temporal resolution of up to 30000 fps, but the area observed in proportion to the vesicles is not particularly useful. We have found a compromise between the

observable area that allows a temporal resolution of 20000 fps.

5. Pipettes

Optical visualization is not sufficient to study the systems of interest. To investigate the interactions of the membranes and ions, and ligands (the cations) and receptors one must be able to quantify the interactions and energies associated with both relationships. The micropipettes are crucial to the work. They are open cylindrical glass capillaries that can be observed and manipulated in the field of view of the microscope. In this work we use micropipettes to manipulate vesicles as well as perform local microinjections on a group, pair, or single vesicle.

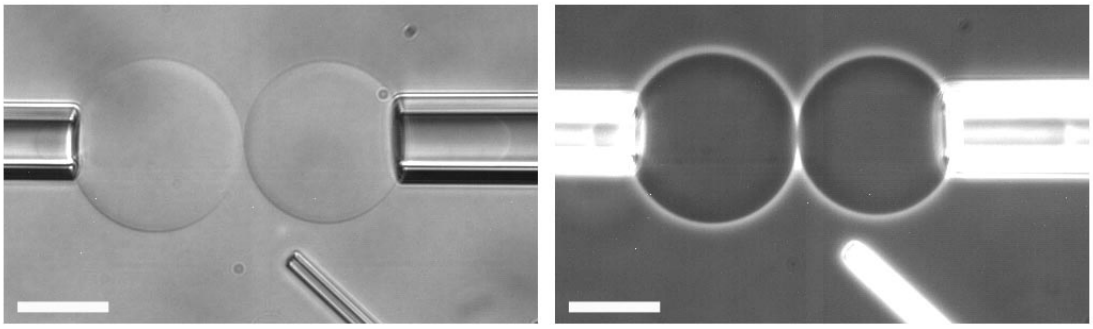

Figure II-4. Under the Microscope: The figure shows two identical images of vesicles being held by micropipettes. The figure demonstrates the difference between images observed using DIC (left) and phase contrast (right) microscopies. The third pipette is the injection micropipette with a inner diameter of approximately 2µm. The scale bar in both micrographs is 20 µm.

The glass capillaries used,1B100-4 (World Precision Instruments, USA), have an outer diameter 1.0 mm and an inner diameter of 0.58 mm, and a length of 100 mm. The pipette is heated in a micropipette puller (Sutter Instruments, USA) and pulled apart forming two pipettes with very fine tips. This tip is then modified by first cutting it with wire cutters to create a tip of the desired size, usually between 5-10 micrometers in diameter. The micropipette tip is then polished using a microforge (Narishige, Japan) making it's end square and giving one more precise control over the finished diameter. The microforge is a thin wire 1mm in diameter coated with borax. One is able to heat the wire it by passing a current through it. This current causes the borax silicate to melt and become fluid like. When the fluid comes in to contact with the glass capillary it is drawn into the capillary. When the heat is turned off, the borax becomes solid again and begins to contract. This contraction induces a tension, causing the capillary to break giving it a flat face. The face is made smooth, melted, by a short pulse of intense heat from the wire at a distance of 200-400

micrometers. Finally, the inner diameter of the finished micropipette tip is 5-10 micrometers. The outer diameter, now irrelevant to the measurement, is between 7-12 micrometers.

One micropipette in the set up is always used for the local injection of the active solution, namely an electrolyte mentioned above. The same type of glass capillary is used to make either micromanipulation or microinjection micropipettes, the only difference being that the injection micropipette has a smaller tip diameter. It has an inner diameter that is on average 2 micrometers. Using micropipette tip with a smaller tip diameter gives one better control over the balance pressure used to control ambient flow in or out of the micropipette. An apparatus, called a picoinjector (Harvard instruments, USA), is used to control the injection of solution in the vicinity of the vesicles.

There are two micromanipulators that are mounted on additional stages bound to the side of the microscope, and one free standing post to hold the injection micropipette. The micromanipulation micropipettes are filled with inert solution identical to the solution in the observation chamber. They are held by two wet chucks (Narishige, Japan) which are connected to their respective pressure sources MP30E, M-500 (Physik Instrumente, Germany), PLI 100 (Harvard Apparatus, USA), and placed into their respective micromanipulators (MP-285 Sutter Instruments, USA), The injection pipette and pipette chuck are mounted into a mechanical manipulator (Narishige, Japan). Once the pipettes are mounted they can be independently positioned axial, lateral, and vertical (x,y,z) directions. the electromechanical micropositioners (SI) have a displacement resolution of 40 nm and the purely mechanical micropositioner (Narishige) a displacement resolution of 250 nm.

The two micropipettes used for manipulation are connected to two vertical linear translation stages which have a displacement resolution of 1 micrometer. These translation stages carry the water reservoirs and, connected to a wet chuck via a 1mm diameter rubber hose, are responsible for the aspiration pressure used to hold and manipulate the vesicles. The movement of the water reservoir (10 micrometers) results in a change in pressure of ±1 dyne/cm^2 (0.1 Pa), displacement of a millimeter

results in a change in pressure of ±100 dyne/cm^2 (10 Pa), the latter is enough to stretch a vesicle membrane The injection pipette is connected to an picoinjector which controls the volume of injected solution using high pressure air. The air pressure can be changed with a resolution of 1 kPa, but the volume of solvent injected is a result of the dimensions of the pipette and length of time that the pressure is applied which has a temporal resolution of 10 ms.

Connected to a water reservoir one is able to create a pressure difference between the inside and outside of the pipette. Using a micropipette this pressure difference can be applied to a giant vesicle and used to aspirate, hold, stretch, and manipulate it. Once a vesicle is held inside a pipette the pressure difference exerts a surface tension on the vesicle membrane. The pressure difference can be varied between 0.1 Pa to 50kPa, resulting in a force exerted on vesicle between 0.1 pN and a 1μN, respectively. The observation chamber has two air water interfaces on opposite sides to allow insertion of micropipettes. The vesicles settle at the bottom of the observation chamber. Due to slow evaporation at the interfaces leads to directed diffusion of the vesicles towards the center of the observation chamber. There they arrange themselves in a close packed configuration. As such we have a "vesicle reservoir" from which to select the appropriate sized vesicles or perform test on large groups of vesicles. Application of force on the vesicle membrane results in a mechanical surface tension, at such forces surface tension must dominate the deformations. When the applied forces are distributed over large surface areas one is able to focus the attention on stretching deformations.

The vesicle is aspirated into a micropipette so that it forms a spherical segment on the outside of the pipette. In a mechanically stable environment a vesicle maintains a constant surface area and volume over a duration of a measurement. The aspirated vesicle is brought in close proximity to the test surface, in this case another vesicle. The electrolyte solution is injected, followed by a release in suction pressure leading to adhesion of the two vesicles. The mechanical analysis of the equilibrium shape provides the ratio of free energy density for the surface affinity to a particular pipette suction pressure (Evans 1980). Details of the actual forces involved in the adhesion process are not observable but are accumulated over the entire surface area. At the

time of the experimental observation the pipettes are stationary, and the pressure is changed remotely from a computer, or a dedicated apparatus. The image can only be viewed from one camera, or through the oculars, at a time. That means that the experimenter is dedicated to one type of experiment (either fusion, or adhesion, or area expansion., or elasticity measurements) depending on his/her needs concerning length, or level of difficulty during of the observation.

It is clear that different techniques used will reveal different aspects of the interaction between ions and the vesicle membranes. Studies on submicroscopic vesicle dispersions will provide us with a molecular picture of the thermodynamics associated with ion-membrane interactions, and the application of light scattering techniques described will shed some light on membrane-membrane interactions induced as a result of the ion-membrane or ligand (cations)-receptor interactions. The micropipettes and light microscopy will allow us to mimic the ITC experiments and directly visualize the changes induced by the presence of the ions. Using the micropipettes we will be able to investigate changes as a result of local perturbations to pure Egg PC lipid, and functionalized, bilayers. In addition the micropipettes will allow us to isolate pairs of giant vesicles and directly monitor differences in mechanical membrane properties that may lead to fusion of the lipid bilayers. Applying the aforementioned techniques will allow us to develop an understanding of how specific molecular recognition influences membrane- membrane interaction and lipid bilayer fusion.

We have engineered a system from a small number of components with which to study model membrane interactions by utilizing specific ligand-receptor recognition. Similar to cell bodies the lecithin bilayer membrane acts as our lipid matrix. By embedding the amphiphilic receptors ß-diketone or bypiridine into a lipid matrix we transform the bilayer into a functional membrane. Using either LUV's or GUV's we can investigate the interaction of the functionalized vesicles on both the nanometer and micrometer length scales. Additionally we govern the interactions between different lipid bilayers, and receptors using multivalent ions. The system is capable of specific interaction through ion mediated coordination and recognition. Using the materials and methods just described, our aim is to observe and characterize

the effect of the inter-vesicle recognition guided by specific ligand-receptor interactions. As such we have constructed a system that has the potential to coordinate specific interaction between two vesicle membranes and the means to characterize the effect of these interactions.

III. Results and Discussion

A. Small Vesicles

1. Titration Calorimetry

We would like to gain an understanding of the molecular phenomena involved in the system. Characterization of these interactions involves the investigation of the energetics of the intermolecular and inter-vesicle interactions. Using isothermal titration calorimetry, and conducting experiments in a controlled way, we are able to break down the interactions involved in the system based on the changes in heat measured in an adiabatic environment. By taking a minimalist approach with regards to the components involved we have engineered a system that will allow us to develop an understanding of the interactions leading to the fusion of membranes. We will compare differences between measurements of the interaction of multivalent transition and lanthanide metal cations in the following systems

- Ion-water interactions, in the absence of vesicles
- Ion-phospholipid interactions, a reference measurement in the presence of pure EPC membranes,
- Ligand (cation) -receptor interactions, membranes functionalized with amphiphilic receptors with ß-diketone and bipyridine functional groups,

Doing so we are able to break the system down piece by piece and develop an understanding of how molecular interactions affect membrane fusion. With direct measurement of the heat associated with these molecular interactions we will be able to determine the enthalpy and affinity of cations for the phospholipids and receptors which make up the vesicle membrane. Such measurements will give us an understanding of the basis of intermolecular recognition and inter-vesicular interaction induced by the presence of multivalent cations. In particular, we will attempt to measure the energetics associated with fusion of PC vesicles as a result of functionalization of the lipid bilayer.

We use ITC to measure the heat produced or absorbed by a reaction. At constant pressure we identify the changes in heat with the thermodynamic quantity enthalpy (*H*). The change in enthalpy is measured as a global property of the entire system. The total heat released contains contributions from the mixing of the two solutions. Interaction in a medium, in our case aqueous glucose solution (0.2M) involves both interactions with glucose and water molecules. By injecting electrolytes into glucose solution identical to those used in our study of membrane-ion interactions we can determine the heat associated with mixing of two solutions plus other nonspecific effects associated with the measurement. Here we averaged the signal measured due to the mixing of 0.010 ml of 2mM europium (III) chloride in glucose into the glucose solution reservoir with a volume of 1.442ml. The magnitude of the heat released (exothermic) due to mixing of the solutions was measured to be 5.6 μcal per 0.010 ml injection. As a note, this was approximately 2 times larger than the heat produced due to the dilution, also exothermic, of 0.010 ml glucose into 1.442ml containing the identical glucose solution and 10 mM Egg PC (EPC) vesicle dispersion. In the end the average signal due to mixing was scaled based on concentration used for a given measurement and subtracted from the measured data (Figure III-1B).

The building blocks of the membrane, phospholipid molecules, have a polar head group but it is accepted that the bilayer surface has a net charge equal to zero. This allows the LUV's to be treated as neutral particles and results in the formation of a stable vesicle dispersion. The size of the vesicles used in the ITC measurements was on average 100 nm in diameter, that is four orders of magnitude larger than the size of either the anions or cations in solution. Just for reference, and to put it on a more tangible scale, that would be like comparing the two radii of curvature one with a 1 cm radius in comparison to another with a 50 m radius. With that in mind the surface of the vesicle appears to be, to a good approximation, planar to the ion. One can also compare the area per head group of a phospholipid molecule which is 0.70 nm^2, with an atomic radius of a given ion used in the measurements, 0.18 nm for a chloride anion, and accepted radii of the cations used in the measurements are measured to be even smaller. Using a lipid concentration of 10mM, and suspended in glucose solution, the vesicle spacing is sufficient to assume no initial interactions between

vesicle membranes. With these considerations accounted for one is able to address the interaction of ions with the phospholipid lipid bilayers.

The ITC experiments performed consisted of injecting 10 µl of a given electrolyte in an aqueous glucose solution into a 1.442 ml volume of solution containing a dispersion of large unilamellar vesicles, having on average a radius of 50 nm, suspended in an isotonic aqueous glucose solution, with a lipid concentration of 10mM. At most, 60% of the concentration of the lipid is considered available for interaction with the injected ions reducing the effective concentration of lipid to 6mM (i.e. the lipid in the external membrane leaflet of the vesicle). The results for a given measurement are shown in the Figure III-1 below. The example given is a result of the interaction of the vesicle suspension with 10 µl injections using an injection solution containing 1mM europium (III) chloride. In the top graph, the raw data, the heat flow was recorded for the duration of the measurement. The spikes in the graph, positive in magnitude, are indicative of an endothermic signal and are the result interaction between the contents of the injection solution and contents of the working cell. Integration of the heat flow with respect to time yields the heat per injection, or the enthalpy due to an individual injection, in this case europium (III) chloride. The graph in the middle of the Figure III-1 compares two separate effects from different ITC measurements, one the heat released as a result of mixing (blue points) and the second the heat released as a result of the interaction between the ions and the lipid (red points). The measurements were made with the same injection solution having identical 1mM $EuCl_3$ concentrations and 10µl injection volumes.

Comparison of the enthalpy due to mixing and enthalpy due ion-lipid interactions shows that the signal is small but not negligible. Subtraction of the two signals results in real signal (dark red points), or real enthalpy due to the electrolyte membrane interaction. The trend of the corrected curve is indicative of the interaction between the cat- and anions in solution and the phospholipid membrane. As the titration begins virtually all of the ligand is bound to the membrane resulting in a larger signal. As the concentration of the ligand increases in solution the area of the membrane left to bind the ligand is reduced. Therefore injection of the same volume of ligand results in a smaller signal. As the system becomes saturated there is no more

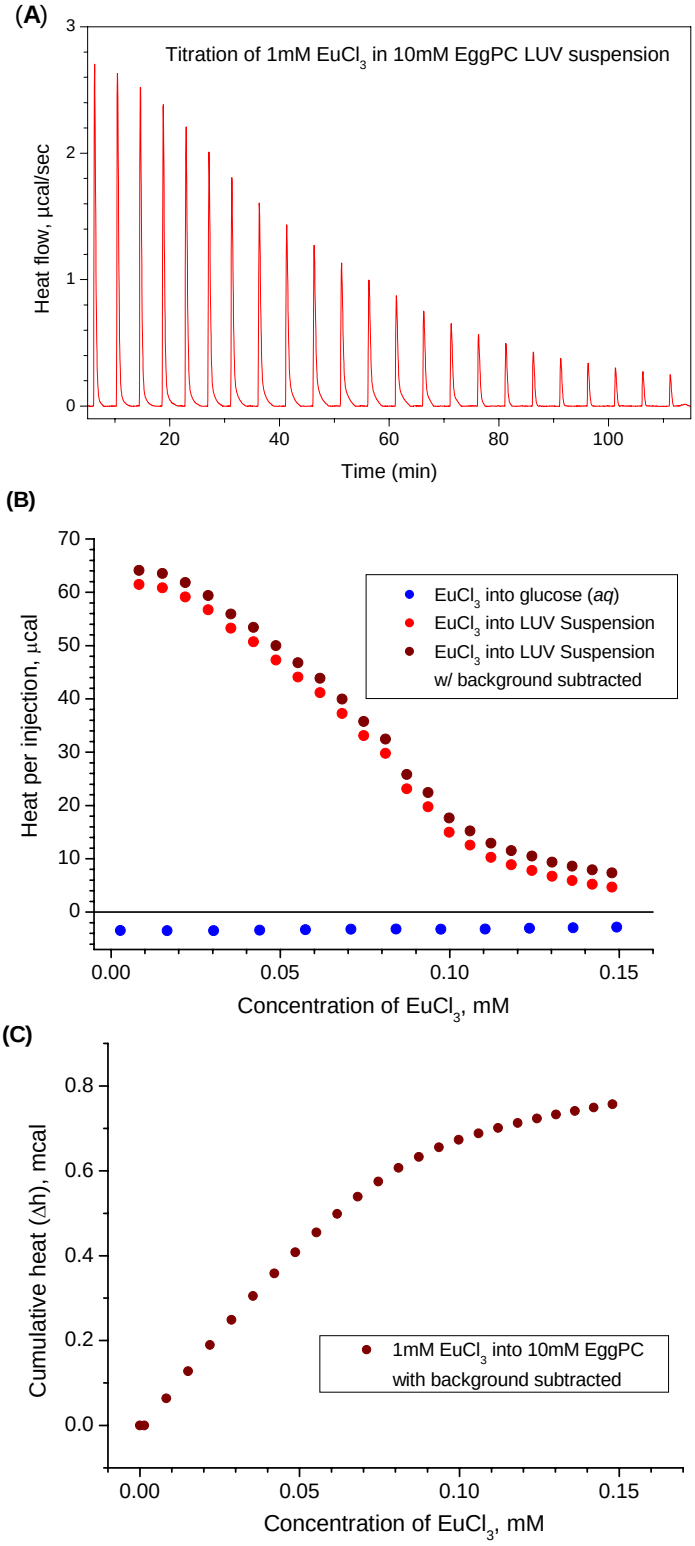

Figure III-1. Plotting ITC Data: The figure shows a sample of the data obtained from a typical ITC experiment where 10 µL aliquots of 1 mM solution of $EuCl_3$ were consecutively injected in 10 mM solution of EPC LUV's. All solutions were prepared in glucose. (A) Raw data as measured by the instrument with baseline subtracted: the heat flow plotted as a function of time. (B) The same data integrated over time: in this case change in heat is plotted as a function of the concentration of salt in the working cell. For comparison the signal obtained from dilution of $EuCl_3$ into glucose, no vesicles present, is plotted on the same graph. The difference between the two data sets gives the heat from interaction of ions with the membrane only. (C) A graph of the integrated heat summed after each injection, yielding the cumulative heat for the measurement.

Membrane left for the ligand to bind to, and the ligand is just distributed equally throughout the solution.

A number of electrolytes were examined as potential ligands to be used to promote the targeted inter-membrane interaction between vesicles. It is known that for vesicles dispersed in ionic solution the affect of the chloride anion is negligible in comparison to the cation-membrane interaction. Two of the electrolytes used $NiCl_2$ and $CuCl_2$ contained divalent ions when dissociated in aqueous solution. ITC measurements using these two electrolytes showed interaction with the vesicle dispersion that proved to be exothermic, and proportional to the signal obtained by mixing of $EuCl_3$ in glucose solution shown in Figure III-1. Due to the weak interaction we chose to direct further measurements and discussion towards membrane ion interactions involving $EuCl_3$. The strategy being that those electrolytes exhibiting the greatest interaction enthalpy would have the greatest potential to induce formation of ligand-receptor complexes, which will in turn effect the properties of the membrane leading to fusion of the bilayer.

We want to know how the molecules interact and why they do so. Based on the description just given the question is, why is there an interaction between a neutral membrane surface and cation? The initial interpretation is that there is an interaction between the ions and the lipid in the membrane. The explanation of the interaction of the zwitterionic membrane and the charged molecules in particular the europium (III) cations is a case of physisorption of the cations onto the membrane surface. The process of physisorption between the molecular surface does not result in a chemical bond, allowing the molecules to retain their molecular identity. As such we are able to identify the ligand and receptor in our current system, where the ligand is the cation, europium (III) in the example above, and the receptors are the phospholipids.

In this ligand-receptor context we are able to investigate adsorption of the ions onto membrane. The models describing adsorption to surfaces assume three conditions;

- adsorption cannot surpass complete coverage of the surface,

- all sites are independent and equivalent,
- the surface is uniformly covered.

The models which we consider applying to describe ion-membrane interactions in our system are presented below.

1) Henry-Dalton equilibrium

The simplest model known in literature describing adsorption equilibrium states, that the amount of adsorbed or bound ions is proportional to the amount of free ions in the system, C_{eq}. The proportionality constant is K, with the units M^{-1}:

$$X_b = KC_{eq} \qquad (1)$$

X_b is a molar fraction of cations bound to the surface vs. all lipid molecules available for interaction:

$$X_b = \frac{\#\, europium\,(III)\, ions\ bound\ to\ the\ membrane}{\#\ of\ lipid\ molecules\ available}$$

and can be expressed as a concentration ratio:

$$X_b = \frac{C_b}{C_L^0}$$

where C_b is the concentration of bound ions, and C_L^0 is the concentration of all lipids available for binding. Equation (1) is referred to as the Henry-Dalton partition equilibrium. According to this model the more ions introduced into the system, the more ions will bind to the membrane without exhibiting saturation. Taking into account the mass conservation law, the free ions can be expressed as

$$C_{eq} = C^{tot} - C_b$$

where C^{tot} is the total ion concentration. Then for the final expression for X_b one obtains,

$$X_b = KC^{tot} / \left(1 + KC_L^0\right) . \qquad (2)$$

Because of the linearity (X_b is linearly proportional to the total concentration of ions), this model suggests that the amount of bound ions is the same for every injection, i.e. the released heat from every injection is the same, which was not observed in our experiments (see Fig. III-1 B).

2) Langmuir adsorption isotherm

The second model that we address is the Langmuir adsorption isotherm. It is one of the most widely used models concerning binding of various molecules and ions to membranes (Altenbach and Seelig 1984; Lehrman and Seelig 1994). The interaction between the lipid (L) and the metal ion (M) can be expressed in terms of the mass action law, written as

$$M + L \leftrightarrow ML\,. \qquad (3)$$

At equilibrium the relationship can be related to the equilibrium constant (K) which also has the dimensions of M^{-1}

$$K = \frac{[ML]}{[M]\cdot[L]} = \frac{C_b}{C_{eq}C_L} \qquad (4)$$

where C_L is the concentration of lipids available for binding, $C_L = C_L^0(1 - X_b)$, (the square brackets in the above equation are standard notation used by chemists to denote bulk concentration). The concentration of the bound ions can be again expressed in terms of the molar fraction X_b leading to

$$K = \frac{X_b}{C_{eq}(1 - X_b)}\,. \qquad (5)$$

For low binding one can assume that the concentration of free ions is approximately equal to the total ion concentration ($C_{eq} \approx C^{tot}$). Then for X_b one obtains

$$X_b = \frac{KC^{tot}}{1 + KC^{tot}} \qquad (6)$$

For larger values of K one has to implement the law of mass conservation which states,

$$C^{tot} = C_{eq} + C_L^o X_b\,. \qquad (7)$$

Using Eqs. (3) and (4) one is able to rewrite the Langmuir model in terms of the fraction of ions bound to the membrane, and other known variables in the system like C_L^o, C^{tot} ending up with a quadratic equation

$$X_b^2 - \left(\frac{1}{KC_L^o} + \frac{C^{tot}}{C_L^o} + 1\right)X_b + \frac{C^{tot}}{C_L^o} = 0\,. \qquad (8)$$

The amount of the ion bound to the membrane as a result of the total concentration of ion in the solution is the root of the quadratic equation

$$X_b = \frac{\left(\frac{1}{KC_L^o} + \frac{C^{tot}}{C_L^o} + 1\right) \pm \sqrt{\left(\frac{1}{KC_L^o} + \frac{C^{tot}}{C_L^o} + 1\right)^2 - 4\frac{C^{tot}}{C_L^o}}}{2}. \qquad (9)$$

The physically relevant root is the one with a '–' sign because X_b cannot exceed 1.

The two versions of the Langmuir model are described in terms of the independent variable, total concentration of europium (III) in the working cell, and the dependent variable, the fraction of europium (III) adsorbed on the membrane. From the figure it is clear that the two models converge at low values of the equilibrium constant. In which case the equilibrium constant describes a low binding affinity of the ion for the surface. For lanthanide ions, the reported values of K are relatively large (Duzgunes, Bentz et al. 1988; Lehrman and Seelig 1994).

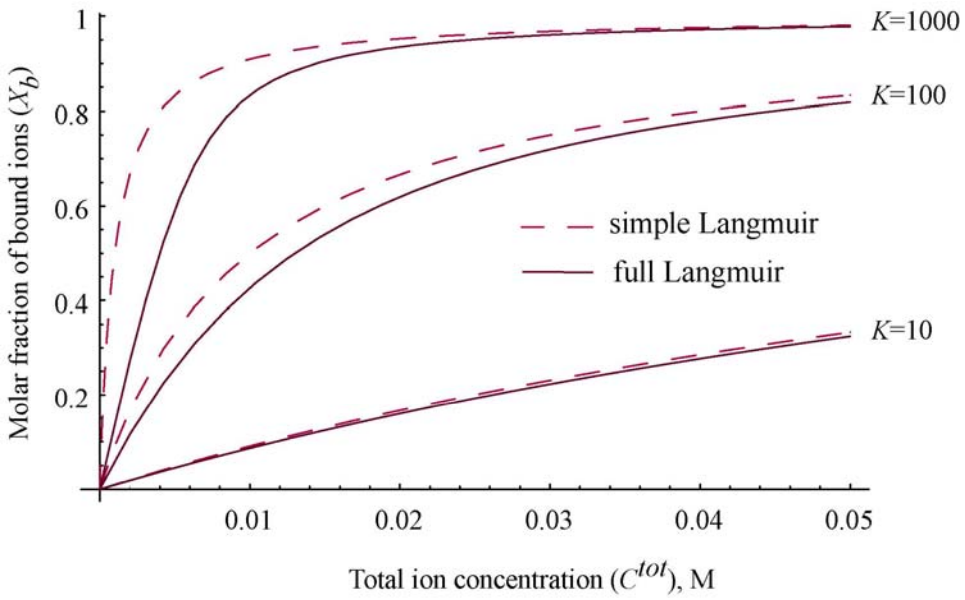

Figure III-2. Result of Simplification: The figure compares the two versions of the Langmuir adsorption model that describe the binding of one cation to one lipid molecule for different binding constants (*K*). The dashed lines are calculated with Eq. (6) and the full lines are calculated using Eq. (9). The lipid concentration was taken to be 5 mM.

3) Ternary binding

Finally, we consider an additional model referred to as the ternary model. Here the adsorption process of the ion to the membrane involves the ion binding to two lipid molecules which written in terms of the mass action equation can be expressed as,

$$M + 2L \leftrightarrow ML_2 . \qquad (10)$$

Because of the stoichiometry of the reaction the lipid available for binding is $C_L = C_L^0(1 - 2X_b)$. Obviously, in this case the maximum value of X_b is not 1, as in the case of 1:1 binding, but 0.5. The equilibrium constant, K, is given by

$$K = \frac{X_b}{C_{eq}(1 - 2X_b)^2} . \qquad (11)$$

For the simple case when $C_{eq} \approx C^{tot}$, for the molar ratio of adsorbed ions one obtains

$$X_b = \frac{1 + \frac{1}{4KC^{tot}} \pm \sqrt{\left(1 + \frac{1}{4KC^{tot}}\right)^2 - 1}}{2} . \qquad (12)$$

If one accounts for the change in the free ion concentration due to adsorption on the membrane (Eq. 3) one obtains a cubic equation for X_b with only one real solution. This solution won't be considered or presented here.

Figure III-3 presents a comparison of the models for a fixed value of the equilibrium constant K over a certain concentration range of ions in the system. To remain consistent in the comparison we find it more appropriate to apply the simplified version of the Langmuir adsorption model with the simplified ternary binding model to our experimental data. The ternary model has been successfully applied to the binding of trivalent cations to negatively charged bilayers containing phosphatylserine (PS) and bilayers made from PC and PS lipids (Duzgunes, Bentz et al. 1988; Lehrman and Seelig 1994).

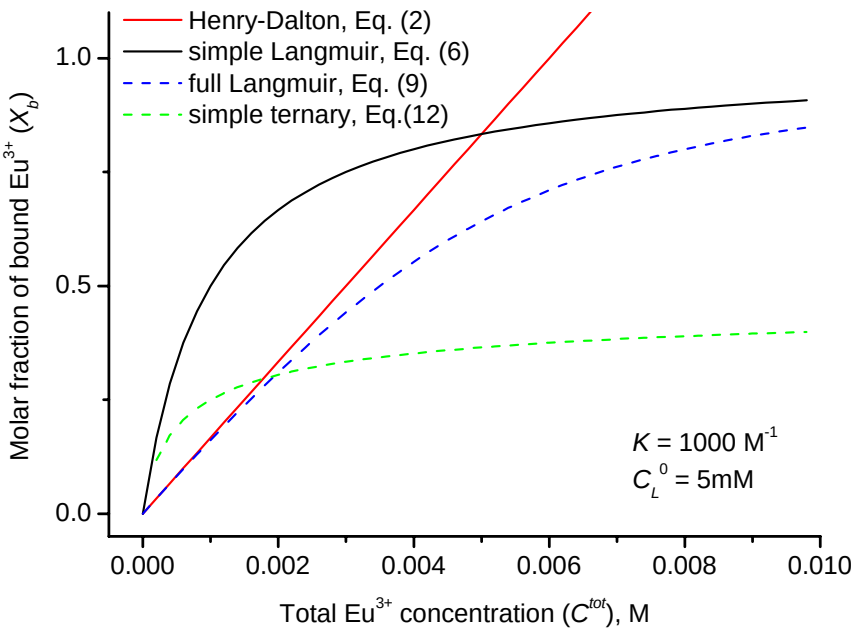

Figure III-3. Binding Model Comparison: A comparison of the models describing adsorption onto surfaces described above. From the experimental data (Fig III-1) it is obvious that the Henry-Dalton model would not accurately describe our data. Finally based on other work and, the properties of the system, we find it appropriate to consider the two simplified models to describe the experimental data measured in our work.

The amount of heat measured is related to the amount of metal bound to the surface according to the following expression,

$$\Delta h = \Delta H \, X_b C_L^o \, V_{cell} \ . \qquad (13)$$

Here ΔH is the enthalpy per mole of europium (III) in the system, V_{cell}, is the volume of the working cell, and Δh is the heat released in the measurement. Summing the heat released as measured in experiment we are able to determine both the molar enthalpy and equilibrium constant in a given measurement by fitting the data with the equation above. In such a fitting procedure we use ΔH and K *(*as expressed in eq. 6 and eq. 12*)* as fitting parameters.

As a first step we can apply the simplified Langmuir adsorption model to the set of data, and use it to determine the both the molar heat of enthalpy associated with the adsorption of the europium to the membrane surface. If K is small enough then we can also apply the ternary model and compare the data obtained from the fits.

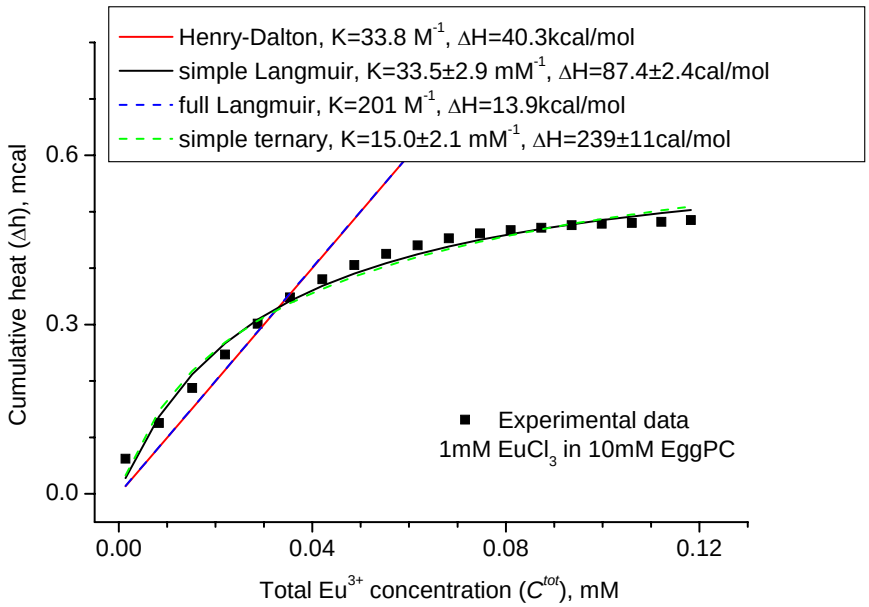

Figure III-4. Applying the Models: The figure compares a typical set of ITC data with the models described above. The values for ΔH and K obtained from the fitting routine are given for each model. It is clear that the full Langmuir and Henry-Dalton models fail to describe the data over the experimental range. Therefore we choose to use the two apply the two simplified models to describe the experimental data.

The errors of the fitting parameters indicated on Fig. III-4 correspond to the fitting accuracy for one measurement. The determination of K and ΔH is more precise if several sets of data corresponding to different concentration conditions are fitted accounting for the experimental error and the reproducibility. Fitting several sets of data simultaneously gives the following results: from the simple Langmuir model $K = 31 \pm 4$ mM^{-1} and $\Delta H = 103 \pm 8$ cal/mol; from the simple ternary model $K = 13 \pm 4$ mM^{-1} and $\Delta H = 283 \pm 33$ cal/mol.

An alternative way of analyzing experimental data obtained for ions binding to membranes has been suggested by Altenbach and Seelig, 1984 . It consists of constructing a plot where selected variables would have linear dependence. For example, if we consider the simple Langmuir model, Eq. (5) suggests that plotting X_b/C^{tot} as a function of X_b would give a linear function with slope equal to the binding constant. Having in mind that the experimentally measured heat Δh is linearly

dependent on X_b (see Eq. 13) one can consider plotting $\Delta h/C^{tot}$ as a function of the released heat Δh, $\frac{\Delta h}{C^{tot}} = K\Delta H - K\Delta h$. This is illustrated in the following figure.

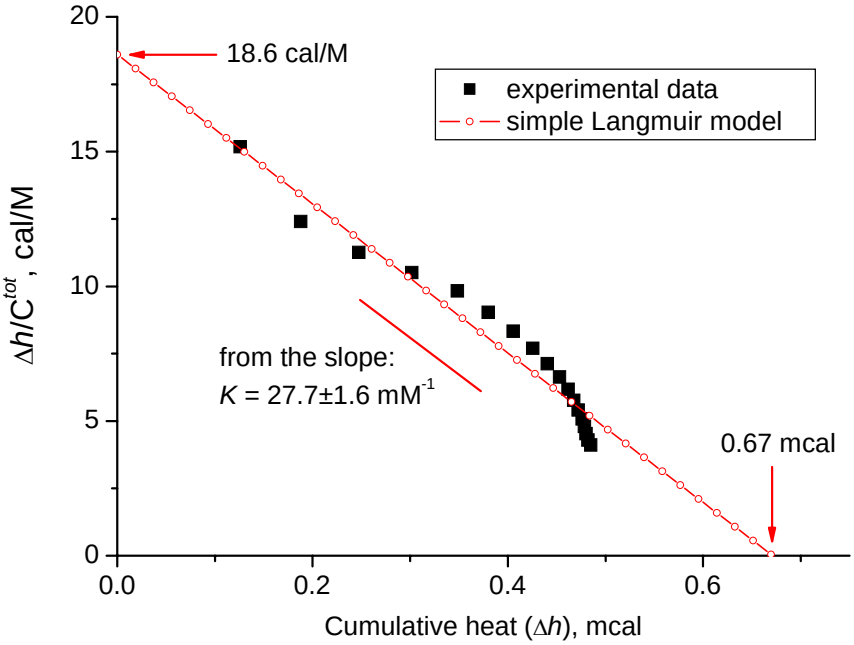

Figure III-5. Alternative Representation: The graph above shows an alternative representation of the experimental data. A plot of the data as $\Delta h/C^{tot}$ vs. Δh and a linear fit to the data yields a K and ΔH near those obtained using simplified Langmuir adsorption isotherm .

The value obtained from the intercept can be used to calculate ΔH: ΔH = 97 cal/mol. The values of both K and ΔH are close to those obtained from fitting the data with the full solution, see Eq. (6).

One can apply similar analysis of the data using the ternary model (see equation 11). In this case one has to plot $\sqrt{\Delta h/C^{tot}}$ as a function of Δh. The slope would yield $\sqrt{K}$ and from the intercept one can extract ΔH. This type of representation, although fast and simple and not requiring a fitting procedure, puts the weight on the data points corresponding to the higher concentration (larger $\Delta h/C^{tot}$). After consideration of all of the different models, and ways to determine the experimental values for ΔH and K, we chose to use the fitting procedure presented in Fig. III-4.

After having discussed the interaction of europium (III) with pure lipid membranes we address the interaction of europium (III) with functionalized

membranes. Here we have incorporated amphiphilic receptors into the lipid bilayer such as β-diketone shown in figure II-4 (pg. 25). Figure III-6 compares two types of measurements: europium interacting with pure lipid membranes (same data set as in Fig. III-4) and europium binding to membranes containing 0.5% (mole) β-diketone. The signal from the latter is still endothermic but with reduced intensity. We determine the real signal due to the interaction of the ligand (Eu^{3+}) with the membrane bound receptor by subtracting the europium (III)-lipid measurement from the signal obtained for the ligand (Eu^{3+}) receptor interaction. From the procedure we find that the difference (open diamonds in Fig. III-6) is negative, i.e. the ligand-receptor binding is exothermic.

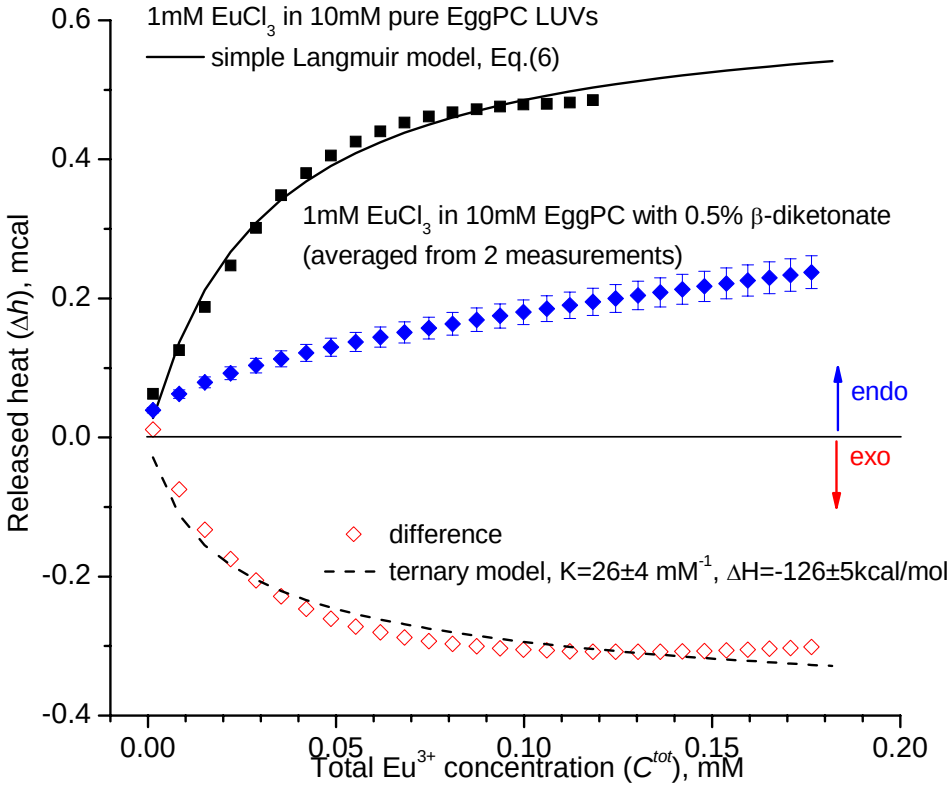

Figure III-6. LUV's, EPC vs. functionalized: The figure is a comparison between the ITC signal measured for the $EuCl_3$ –PC membranes (black) and $EuCl_3$ with functionalized membranes (blue). The difference is the signal as a result of the ligand receptor interactions i.e. Eu^{3+} ß-diketone.

The analysis of the ligand-receptor interaction was performed in a similar way as in the case of metal-lipid interaction. The difference being in the fitting formulae (Eq. 13) one must account for the molar fraction of receptor, $n_{receptor}$, present in the

bilayer, not the concentration of lipid. (the measurements shown here the receptor concentration is 0.5% of the total lipid concnetration):

$$\Delta h = \Delta H \, X_b n_{receptor} C_L^o \, V_{cell} \qquad (14)$$

Considering that one europium (III) ion is capable of forming a complex with more than one β-diketone receptor (Lehn, Sabbatini et al. 1993) it is reasonable to expect that the ternary model would be the most appropriate for analyzing the ligand receptor interaction. The fit is displayed on Fig. III-6. The obtained value for the binding constant is similar to the case of metal-lipid interaction. However the determined reaction enthalpy in this case is orders of magnitude higher: ΔH = 126 kcal/mol. This is not surprising because coordination bonds are characterized by energies of similar magnitude. Our conjecture, based on other work with ß-diketone, (Bauer, Blanc et al. 1964; Marchi-Artzner, Brienne et al. 2004) is that more than one ß-diketone receptor forms a complex with a single Eu^{3+} ligand. The results obtained here for ΔH, a factor of two greater than general coordination chemistry bonds (60 kcal/mol), suggest that the ligand-receptor complex occurs in a 2:1 ratio (2 ß-di. molecules for one cation). This agrees with experimental results obtained independently in the references above.

The binding constant of the two processes discussed above can be used to extract the standard free energy of europium partitioning between the water solution and the membrane (whether pure or functionalized) (Heerklotz and Seelig 2000):

$$\Delta G = -RT \ln 55.5K \qquad (15)$$

The factor 55.5 corresponds to the molar concentration of water and is introduced to keep the equation dimensionally consistent (essentially all concentrations should be given as mole fractions with respect to water rather than by mol/l). Then for the Gibbs free energy for europium binding to EggPC we obtain −8.5 kcal/mol (we use the value of K obtained with the simple Langmuir model) which is of the order of 14 k_BT. Since the measurements were performed at constant pressure and temperature, the processes which occur must be characterized by a negative change in the Gibbs free energy: $\Delta G = \Delta H - T\Delta S < 0$, where T is the temperature and S is the entropy. For

endothermic processes, this implies a large change in entropy $\Delta S > \Delta H/T > 0$, i.e., the driving force for the ion-membrane interactions is a gain in entropy. Because the measured reaction enthalpy is negligible compared to ΔG, the entropy term $T\Delta S \approx \Delta G \approx 14\ k_B T$.

2. Light Scattering

Dynamic light scattering (DLS) is another non-invasive and accurate method for characterizing lipid vesicle dispersions. Light scattering techniques are able to characterize the homogeneity of vesicle size and shape or the contrary, polydispersity (Van Zanten 1996). Here we apply light scattering to compliment the ITC measurements and use it to determine the interaction, adhesion or fusion, between vesicle as a result of membrane-ion or ligand-receptor interaction.

Vesicle sizing was performed for every ITC measurement investigating the interaction between ions and membranes these were measurements made on; pure Egg PC LUV's, LUV's functionalized with ß-diketone and bipyridine receptors having various membrane receptor concentrations, and using various electrolytes and electrolyte concentrations. Typical results obtained from the DLS measurement are shown in Figure III-7. Each of the two graphs display one curve for the vesicle size distribution before the ITC measurement, i.e. with no electrolyte present. The distribution of vesicle sizes is narrow and centered around an average vesicle radius of 50 nm, that corresponds to the final pore diameter (100 nm) the vesicle dispersion was filtered through in the extrusion process. Also on each graph there is a trace for the particle size distribution measured after the ITC measurement, i.e. with electrolyte. This trace corresponds to the result of 30 injections of electrolyte into the vesicle dispersion in 10 µl aliquots. The distribution of vesicle sizes noticeably increased. It should be noted that both aggregation and fusion contribute to changes in light scattering intensity. Therefore increase in radius can be attributed to either adhesion or fusion between vesicles. A decrease in vesicle size can be attributed to membrane rupture and reformation of the bilayer into smaller vesicles, or membrane rupture leading pore formation and leakage of the membrane contents, loss of lipid, or both, resulting in smaller vesicle sizes

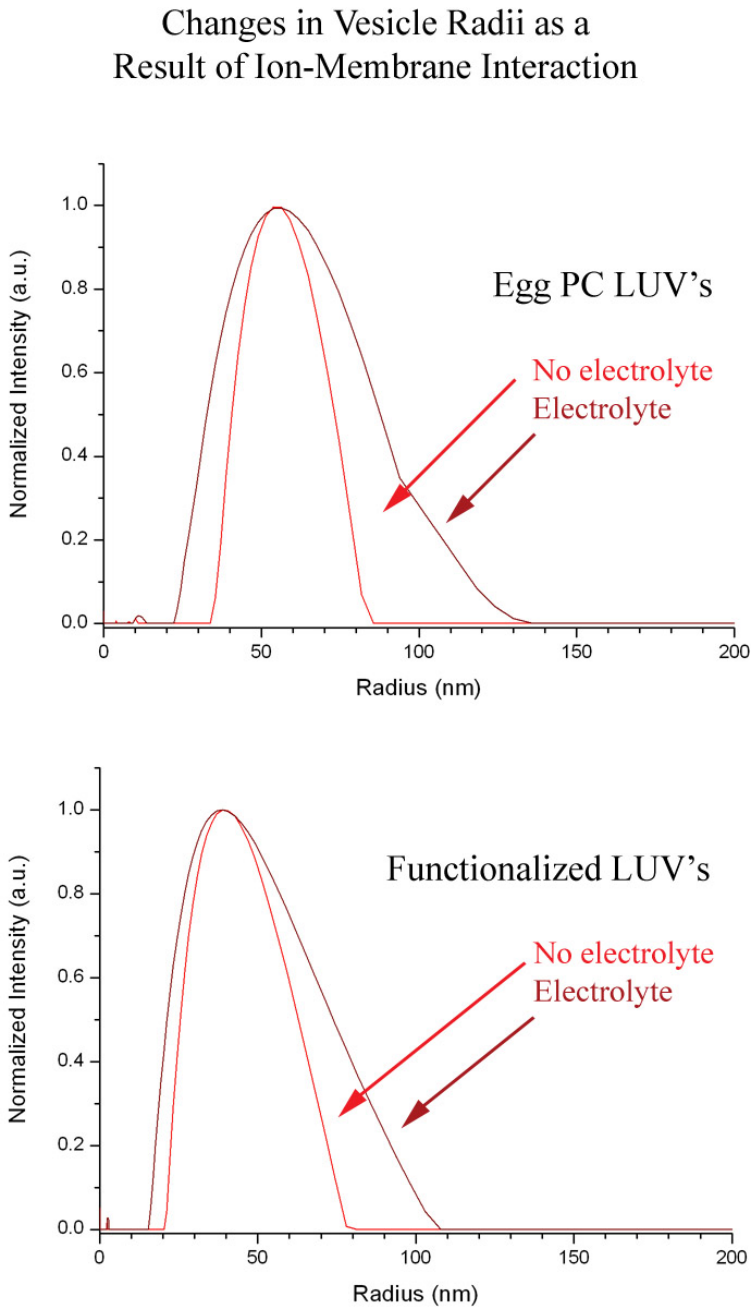

Figure III-7. LUV Size Distributions: The two representative graphs describe how vesicle size distribution changes as a result of injection of electrolyte solution. The measurements were made before and after each ITC characterization. All traces show a mean vesicle radius ≈ 50 nm. A comparison of the two graphs show similar behavior, a broadening of size distribution 25% for Egg PC LUV's and 14 % for functionalized LUV's. Due to the similarity in the results before and after addition of ions it is difficult to draw conclusions based on the functionalization of the membrane. On the other hand, there appears to be a significant change in vesicle size as a result of the addition of ions.

Over 20 sets of light scattering measurements were performed and analyzed for changes in vesicle size. From theses measurements no definitive conclusions could be drawn with respect the changes in vesicle size distribution resulting from injection

of different electrolyte solutions. That is, from all of the permutations of injection concentration used, in particular 10 mM, 5 mM, 2mM, and 1mM $EuCl_3$, and comparison of the results between LUV's extruded with only Egg PC versus LUV's functionalized with either ß-diketone, or bipyridine receptors, the changes in vesicle size distribution on average were measured to increase less than 20 % of the original, as demonstrated in Figure III-7. To shed some light on the interactions induced as a result of the electrolyte injection we will redirect the focus of this work towards the observation of vesicles using light microscopy and mechanical manipulation of the membrane using micropipettes, where the affect of the electrolyte-membrane interaction can be directly observed. Based on the results obtained from the ITC and DLS measurements we will concentrate on investigations using only $EuCl_3$ and functionalized vesicles bearing ß-diketone receptors.

B. Giant Vesicles

Experiments with giant vesicles involve taking a step back from making measurements in a black box on a large number of vesicles. We trade the shear number of interacting species for a larger surface area per vesicle, which translates into a large working area for interaction between the membrane surfaces and molecules. Giant vesicles have a radius that is greater than 5 microns, easily visible using optical microscopy. Here the primary experimental technique used to follow their behavior and induce their interactions is the combination of optical light microscopy and series of micropipettes. One micropipette is used to perturb the local environment surrounding the vesicles and other micropipettes are used to monitor changes in vesicle surface area. Microscopy is applied for direct observation of the interaction of membrane with surfaces, such as other membrane lipid bilayers or glass surfaces, in real time. The optical microscopy set up compliments the ITC and light scattering experiments nicely. As such it will bring the results obtained using the ITC and light scattering into focus, and observations made here will allow us to develop a better understanding of what is taking place in the system.

The set up concerning the microscopy study was described in materials section but we will repeat some of the details here. The vesicles contain sucrose on the inside

of the membrane. In this case the sucrose solution provides enhanced optical contrast of the vesicles when viewed using phase contrast microscopy. In addition to the enhanced contrast, the difference in density between sucrose and glucose results in the vesicles settling on the bottom of the observation chamber. Finally one can use differences in concentration between the inside and outside of the vesicle to reduce its volume and put it in a tensionless state.

Over time the giant vesicles collect into a close packed environment at the center of the observation chamber, a vesicle reservoir, where the spacing of the vesicles is below the resolution of the microscope. The aqueous glucose environment that fills the observation chamber acts as a reservoir for the local injections of electrolyte solution. The diameter of a chloride ion is approximately 0.1 nm, this in comparison to the typical diameter of a giant vesicle, 10 micron, is infinitesimal. Five orders of magnitude, in real terms is the comparison between a sphere with diameter 1mm to that of one with 100m (the length of a football field). The size of the glass surface on which the vesicles rest, has a lateral dimensions on the order of 10 mm, that is eight orders of magnitude larger than the diameter of the ions and three orders of magnitude larger than the vesicle diameter, therefore it can be treated like an infinite plane.

In order to mimic the ITC measurements on a optical scale and visualize the interactions between vesicles as a result of electrolyte injections we can perform experiments using a single micropipette. After approximately 30 minutes the vesicles begin collecting on the bottom of the observation chamber. Over the course of a measurement they settle into the close packed environment described above (figure III-8). In this arrangement the spacing between neighboring vesicles is below the resolution of the microscope (1 micron) and the separation and independence of the vesicles can be questioned. Careful tests were made to prove the GUV's were independent from one another. First, the preparation procedure includes removal of the vesicles from the electroformation chamber and transfer into a separate container, and finally under the microscope through individual displacement of the vesicles using micropipette manipulation. No codependent motion could be observed as a result of the mechanical displacement of individual vesicles.

To study the effects of the receptors on the vesicles we researched four different systems.

Single component GUV's
i) Pure lipid (EPC) vesicles, without receptor

Two components GUV's
ii) Lipid (EPC) plus ligand, molar ratio of 0.5% (lipid: receptor 200:1),
iii) Lipid (EPC) plus ligand, molar ratio of 5.0% (lipid: receptor 20:1)

Multi-Component GUV's
iv) Complex system; lipid, cholesterol, ligand, PEG-lipid, when receptor is present in the membrane in a molar ratio of 5.0% (lipid: cholesterol: ligand: PEG2000-DMPC 42:42:5:1)

Due to the fact that the concentration of the injection solution is undetectable at the mouth of the injection pipette there was a need to perform reference measurements similar to those performed when carrying out the ITC measurements. This is also consistent with the goal of mimicking the ITC measurements. Following this direction, injection of glucose into the neighborhood of the a group of vesicles is highly dependent on the pressure with which the injection solution is expelled from the pipette as well as the position of the pipette with respect to the vesicles. The end result is that the pressure, when great enough (≈ 5kPa), and applied for a long enough time (greater than 10 seconds) acts to displace the vesicles from their resting position. With regard to concentration, as described earlier, differences in concentration resulted in changes in a vesicle's volume through displacement of water across the bilayer.

1. Single Component Lecithin GUV's: Membrane Adhesion and Membrane Failure

The second set of measurements is demonstrated in Figure III-8. The measurements are based upon interactions of vesicles with pure EPC membranes. In an attempt to mimic the ITC measurements only one micropipette was used to inject a given electrolyte into a collection of vesicles. The set of experiments in regard to injection of electrolyte can be subdivided into two groups with respect to valency of the ions, divalent and trivalent (i.e. Ni^{2+} or Cu^{2+}, and Eu^{3+} or Gd^{3+}), the counter ions in the system were always the same (Cl^-). Consistent with the results from the ITC data the injection of Ni^{2+} and Cu^{2+} at a concentration below 1 mM showed no effect

on the stability or aggregation or fusion of the pure EPC membranes. On the other hand the injection of the electrolytes with trivalent cations Eu^{3+} and Gd^{3+} had a dramatic effect on the interaction of the vesicles with one another and the glass surface.

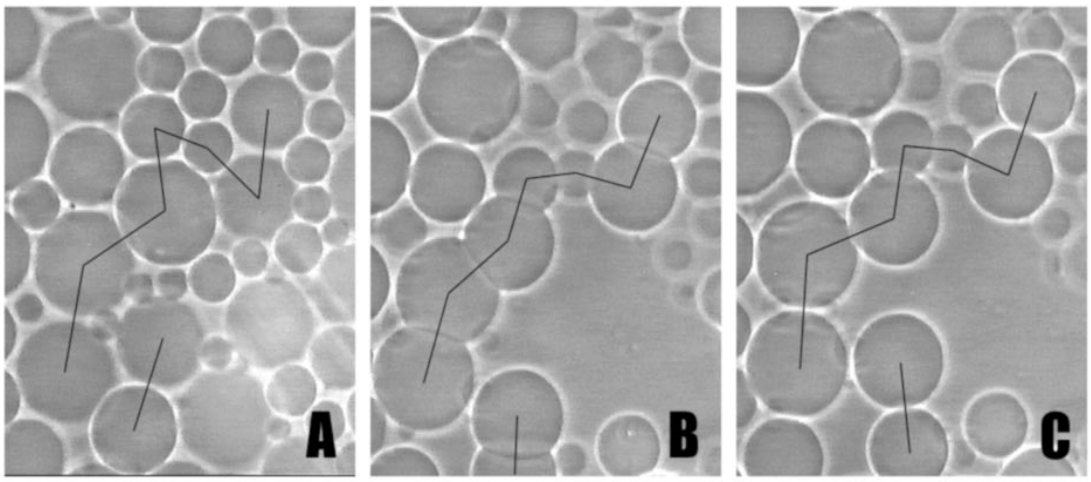

Figure III-8. Transient Adhesion: The image is 110 µm in length. These micrographs show a collection of independent Egg PC GUV's in a closed packed environment, and their response to an injection of $EuCl_3$. Image A, at 0 seconds, shows GUV's before the injection. B, 20 seconds later, shows the interaction between the GUVS as a result of the injection. C, 80 seconds later shows the reversibility of the adhesion induced by the vesicles, returning to their normal independent state. The line is imposed on the picture to indicate which vesicles interact.

The figure above demonstrates the general result of injection of electrolytes with trivalent cations into a closely packed solution of vesicles. The times associated with the micrographs in the figure are A= 0, B= 20, and C = 100 seconds, respectively. As viewed using phase contrast microscopy, the first image labeled A shows the state and arrangement of vesicles in the close packed configuration just before an injection takes place. The shadow of the injection micropipette, positioned slightly above the plane of the vesicles can be viewed in the bottom left corner of the image. The black line imposed on the image is to be used as a guide to the eye, to illustrate the interaction between a collection of vesicles. On short time scales, below one second, the initial effect of the injection is displacement of vesicles in the immediate area surrounding the injection micropipette. It can be concluded from the description and tests described in the subsection above that this is a result of release of the electrolyte solution from the pipette. The second affect of the ions can be observed by comparing the set of images in Figure III-8.

After one second the flaccid vesicles close to the glass surface became tense and adopted a spherical form, and the membranes began to adhere to one another. After 4 seconds over four of the vesicles with smaller diameters (~4μm) disappeared from the area located nearest to the end of the pipette where the electrolyte solution is injected. This is shown in a comparison between picture A and B having a time difference of 20 seconds. In addition to the displacement due to the injection, the rupture of the bilayer membrane is indicated by the void in the area directly below the position of the micropipette. Adhesion between vesicles is indicated by the formation of a train of adhered vesicles in the center, and another pair of adhered vesicles at the bottom of the image labeled B. Finally after waiting a sufficiently long time, in this case 80 seconds (image C). The interaction between the vesicles proved to be transient, and the train of vesicles disassembled.

Further measurements investigating the interaction of vesicle membranes induced by the injection of trivalent cations revealed the details of the processes mentioned above. Using a three micropipette configuration, as illustrated in the methods section (Fig. II-9 pg. 37), we were able to show that the adhesion between a pair of vesicles is induced as a direct result of the injection of ions. In addition we are able to show that the adhesion of vesicles as a result of a local injection of ions within a range of 50 μm from a vesicle contact area is completely reversible. This is done by aspirating two vesicles with excess area into two micropipettes positioning them in contact with one another, maneuvering the injection pipette near the contact zone and injecting nanoliter volume of the electrolyte into the region of interest. After observing the adhesion area decrease to zero, identical in appearance as before the injection took place (t ~ 30 seconds), the membranes were displaced in opposite directions. No membrane deformation occurred, and no effects of adhesion were observed as a result of displacement of the two vesicles.

A combination of epifluorescence and reflection contrast interference microscopy (RICM) were used to discover that the rupture of the lipid bilayer resulted in spreading of membrane onto the surface of the glass. RICM is a technique used to reveal interaction of membranes close to the surfaces. In our system the observations showed a sudden increase in vesicle membrane area close to the glass surface after

injection of electrolytes containing trivalent cations. In addition to the RICM, observations on vesicles with fluorescently labeled lipid were used to confirm the conclusion that the membrane bilayer spread on the surface of glass after failure of the lipid bilayer. After lysis the fluorescent label lipid could be observed on the surface of the glass covering an area greater than the contact area for a vesicle of a given size.

The conclusions that can be drawn from of the series of experiments involving the interaction of electrolytes and pure Egg PC vesicle, based on a number of similar experiments using the above mentioned ions is that there is a clear difference in the interaction of vesicles as a result of the injection of ions dependent on valency of the cation. At low concentrations on the order of μM trivalent cations induced the behavior described above, causing reversible adhesion between neighboring vesicles or the glass surface, and failure of the lipid bilayer, finally resulting in the spreading of the bilayer onto the glass surface. Divalent ions, however, seem to have little or no effect on unfunctionalized vesicles in the millimolar concentration regime, let alone the micromolar regime.

In such a system where injections of an electrolyte are performed in a vesicle dispersion, or locally in the case of giant lipid vesicles, the dissociated ions only interact with lipid molecules on the outside of the bilayer membrane. In solutions that equates to the presence of trivalent cations and monovalent anions. The polar head group of a PC molecule has both a positive charge located on the choline moiety and a negative charge located in the phosphate group. From an electrostatic point of view the interaction of multivalent cations and anions with the lipids in the bilayer must be different. Free of hydration shells, one can envisage chloride anions are capable of interacting with only one positive charge on the choline moiety. Where as a trivalent cation like europium (III) is capable coordinating more than one phosphate group in the lipid bilayer. When ions approach the membrane the difference in electrostatic interaction may induce enough of an instability in the lipid bilayer, i.e. an effective local tension, which can lead to membrane failure.

2. Two Component Functionalized GUV's: Fusion

Furthering the attempts to understand the interactions that take place inside the isothermal titration calorimeter we investigate the response of functionalized giant unilamellar vesicles as a result of micropipette injections. Vesicles mentioned in this part of the work were electroformed from a mixture of egg PC and the amphiphilic receptor molecule in aqueous sucrose solution. Before observation they were mixed with the pure glucose solution and allowed to settle at the bottom of the chamber. Here the focus of the experiments has been placed on observations of vesicles with ß-diketone receptors in the membrane. The strategy being that increased concentration of receptors solubilized in the membrane would result in increased interaction between neighboring vesicles. Two concentrations of receptors were used in the initial experiments, 0.5 % (mole) and 5.0 % (mole) ß-diketone were incorporated into giant unilamellar vesicle membrane. Results from a measurement made with a single micropipette used for injection of the electrolyte into a close packed collection of vesicles are shown in below.

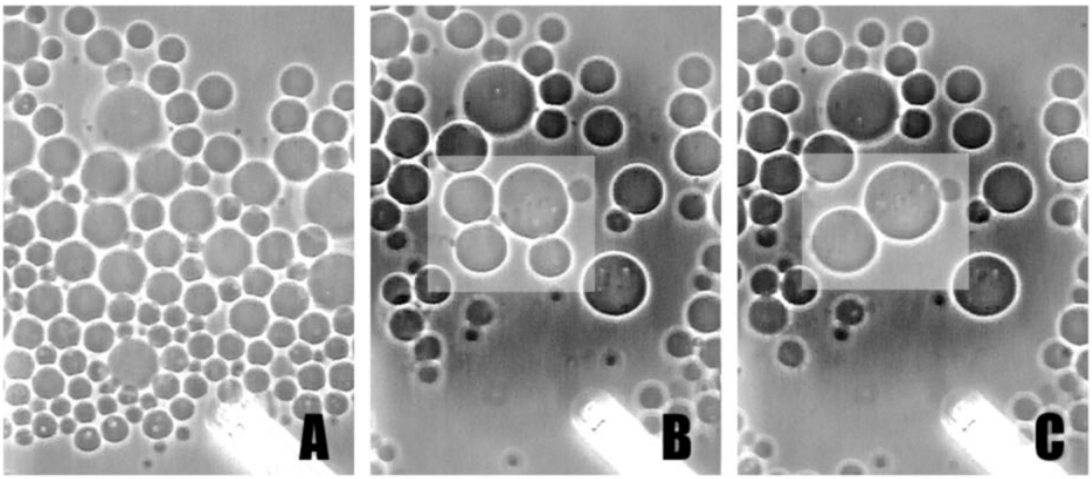

Figure III-9. Membrane Fusion and Failure: The figure shows a collection of independent vesicles functionalized with the ß-diketone receptor in a closed packed environment. The time interval between the images is 60 seconds. Image A (0 sec) shows the initial conditions. In the caption there are approximately 125 vesicles. B after the injection (60 seconds) there are approximately 70 vesicles and 13 fusion events have taken place. C, 120 seconds after the injection there are approximately 65 vesicles, proof of fusion is shown to the left of the highlighted square. The long axis is 220µm .

The figure contains three phase contrast images which are separated by an interval of 60 seconds, i.e. A = 0, B = 60, C = 120 seconds. The first image shows the starting point for measurement. The micropipette used for injection is located in the

bottom right hand corner of the micrographs. There were approximately 125 vesicles located in an area of 40 x 10^3 μm^2 before the injection of europium (III) chloride took place. GUV displacement, inter-vesicle adhesion, and adhesion of the lipid bilayer to the glass surface were all observed. Residual effects due to displacement of vesicles, inter-vesicle interaction, and interaction of the vesicles with the glass surface were identical to those described earlier. In addition to observations just mentioned inter-vesicular fusion was also recorded. Comparison of the images labeled A and B show a sharp reduction in the number of vesicles observed in the area of the figure. During the first 60 seconds there was a reduction of approximately 50 % of the vesicles located in this area. Of those vesicles 13 fusion events were recorded, with nine fusion events taking place in the first thirty seconds after the europium (III) chloride was injected and four fusion events between 30 and 60 seconds. Comparison between the images labeled B and C show little change but attention should be focused on the high-lighted box in the center of the picture

In this region two changes can be detected. The most obvious is that the number of giant vesicles has decreased from four to two. In the last sixty seconds one of the vesicles, located in the lower right corner of the box, has ruptured and spread onto the glass surface. The two vesicles to the left side of the high-lighted area have fused to form one vesicle. These changes can be detected in the picture by a comparison of the remaining vesicle's position and size. The vesicle on the right has not undergone any physical change, in either position or size, where as the vesicle on the right has undergone both changes in position and size. Comparison of figures demonstrates the changes. Both vesicles on the left had a diameter of 25 μm in figure B, in figure C the diameter of the fused vesicle is 32.6 μm. That is a 30 % increase in linear dimension of the two vesicles which is consistent with volume conservation of the vesicle contents during the fusion event. From the results of experiments performed on functionalized vesicles it can be inferred that vesicles with receptor incorporated into the bilayer membrane are responsible for fusion between two vesicles.

The observation of fusion between vesicles warranted more investigation via micromanipulation using three micropipettes and detailed image analysis. In order to perform the measurements two micropipettes were used to hold vesicles in opposition

to one another (Figure III-10). The vesicles were isolated from the vesicle reservoir and held well above the surface of the observation chamber in order to eliminate any nonspecific interactions induced by surrounding vesicles or the glass surface. The third pipette was brought in, placed at an angle, and the solution injected. Systematic measurements were carried out varying the concentration of the membrane bound receptor and europium (III) concentration without a noticeable increase or decrease in number of fusion events observed. In addition, due to the varying time scales which fusion was observed to take place after the injection of $EuCl_3$ into a close packed environment, sometimes as late as 300 seconds, it was unclear how long one must wait before a fusion event would be recorded in an isolated environment.

On several occasions the successful documentation of a fusion event of a pair of isolated functionalized vesicles was recorded. Due to the short time scales over which fusion of lipid bilayers is thought to occur, use of a high speed camera with temporal resolution of 30 μs was employed to catch a fusion event. Figure III-10 shows the difference between a fusion event captured using normal recording rates (25 fps) and one using a high speed camera. In Figure III-10a it is clear that most of the details of the opening of the fusion pore take place within the first two frames of figure. As such one is only able to observe gross changes in the fusion event, and the details of opening of the fusion pore are lost. What takes place in the first 0.04 seconds of membrane fusion is shown in figure III-10b. It clear to see the information one gains from recording using the high frame rates.

Recording with a rate 20000 fps, these eight frames demonstrate what takes place in the first 30000 μsec (0.03 sec) of a fusion event. The first five images show how the membrane pore opens after in the first 200 μsec of a fusion event. The last three pictures demonstrate how the membrane shape and fusion pore continue to change in the next 30 milliseconds. Comparison of the first two images from figure III-10a, and the first and last images from III-10b, indicate that the opening of the fusion pore is similar between the two separate events. In particular one is able to document how fusion pore opens and the inter-membrane adhesion area changes with time. Changes in the inter-membrane contact area are followed by the arrows in each figure. From image analysis of a fusion event recorded with a high speed camera one is able to track how the fusion pore develops.

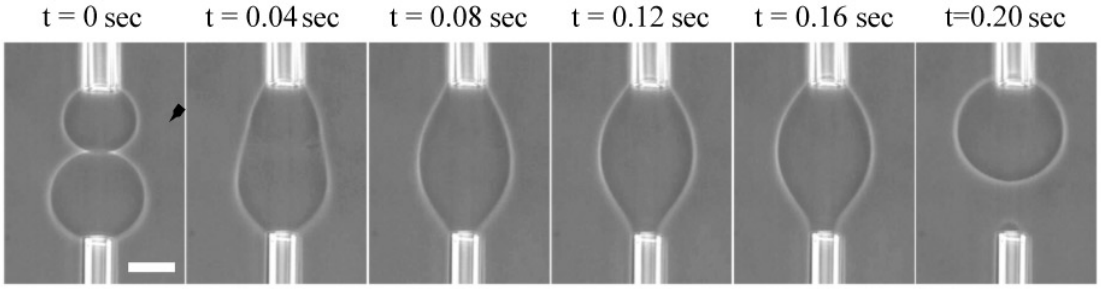

Figure III-10a. Normal Recording: The time series of images shown above demonstrates the temporal resolution available using normal recording rates (24 fps). In the first image, t=0, the black arrow indicates the position of the micropipette used for injection of 50 µM $EuCl_3$ (scale bar = 20 µm).

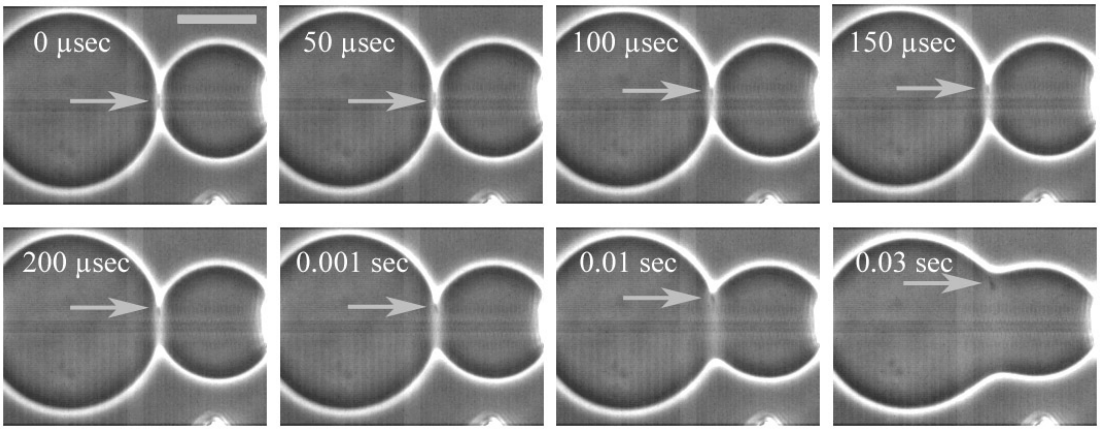

Figure III-10b. High Speed Recording: Comparison of two sets of time images, 10a and 10b, shows the difference in temporal resolution when a fusion event is observed using normal and high speed (20,000 fps) recording rates. The eight images shown in 10b would not be accessible using normal recording rates. The arrow follows the membrane defect associated with the adhesion area before the bilayers fused. In the first image, 0 µsec, the micropipette used for injection of 50 µM $EuCl_3$ is located in the bottom right of the micrograph (scale bar = 20 µm).

Figure III-11 shows one example of membrane fusion and how image analysis is used to discover the opening of the fusion pore. Concerning the analysis, it is extremely helpful to have seen the entire fusion event take place. The series of images are recorded in 50 µsec intervals for entire fusion process. Here only the first 5 frames are shown to demonstrate how image analysis of the membrane contact area complements the images to reveal when the initial steps in membrane fusion begin. The three columns give a different perspective on membrane fusion; an overview, as seen in the full scale images, a close-up of the inter-membrane contact area which is blown up in scale four times, and finally the line profile of the inter-membrane contact area.

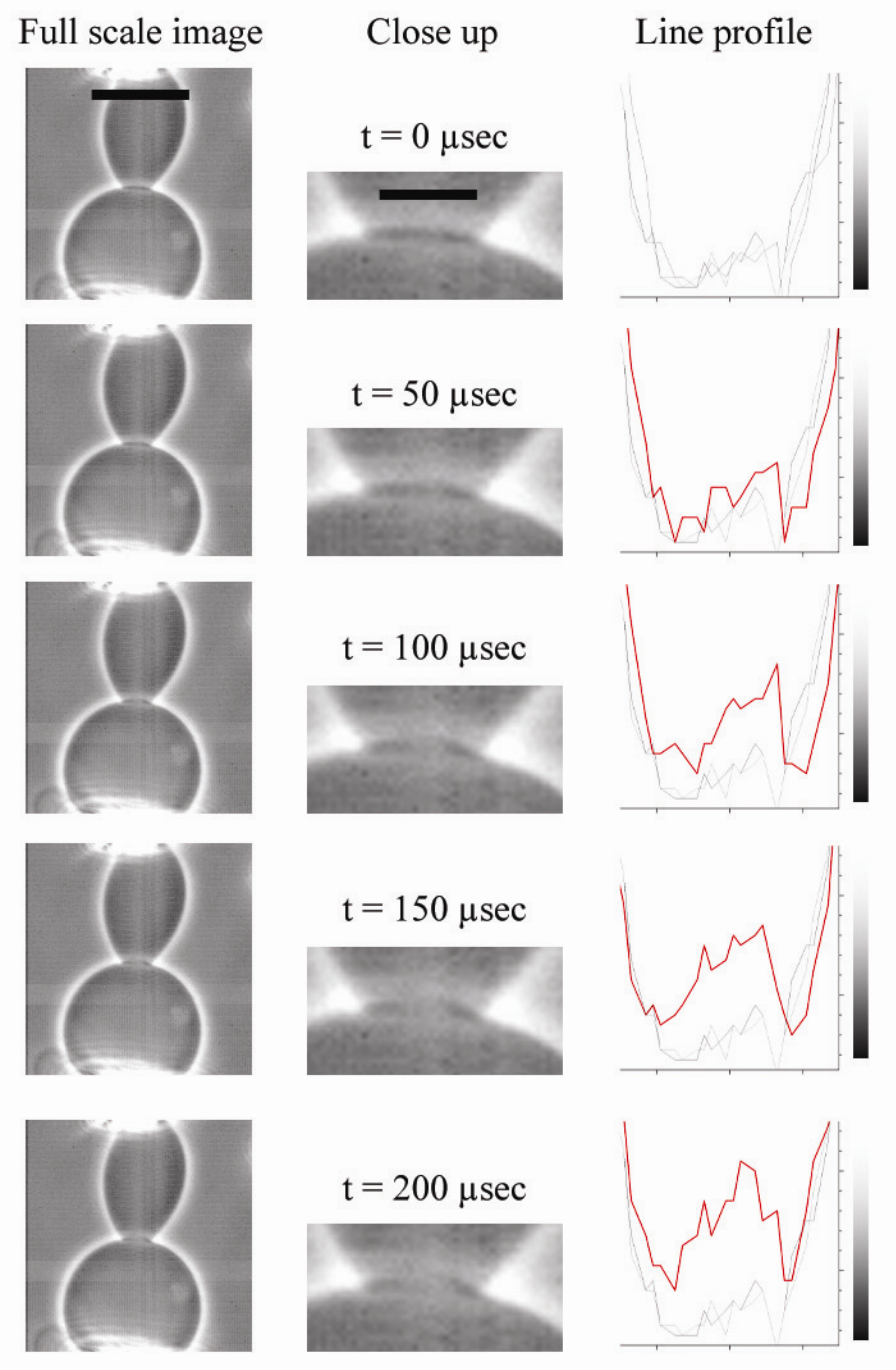

Figure III-11. The Fusion Pore: The figure demonstrates the opening of the fusion pore captured at 20,000 fps; Left, a view of the complete area recorded (scale bar = 20 µm), Center, a close up of the inter-membrane contact area and the times associated with the each frame in the columns (scale bar = 5 µm). Right, Analysis of the gray values associated with adhesion zone demonstrating the the development of the fusion pore in the first 200 µsec.

The line profile of the adhesion area is a measure of the gray values in an image with white measuring 256 and black having a value of 1, i.e. lighter > darker. The membrane contact area is always darker than its surroundings, as shown in the figure. In the image analysis the baseline, line profiles of images analyzed at -100, -

50, and 0μsec are shown in gray, and changes in the baseline are shown in red. The changes in the baseline are used to indicate the onset membrane fusion. A close comparison of the line profiles and the close up of the membrane adhesion area demonstrate how the line profiles are used to reveal opening of the fusion pore. The increase in the line profiles show that the initial change after 50 μsec is small. In the image it is nearly impossible to detect. After 100 μsec the opening of the fusion pore can be visualized in the image, and the change in the line profiles has intensified. It becomes clear that the inter-membrane contact area remains intact despite opening of a fusion pore. Similar to what is observed in Figure III-11b. Complete analysis of the fusion pore will reveal details of the fusion process not observed before.

In order to analyze the process of fusion one must perform a detailed analysis of the entire set of images recorded from a successful measurement. As an example the results from the complete analysis of the fusion event in Figure III-10b will be described here. Similar to the Fig. III-11, an intensity profile of gray values in a line passed directly over the contact zone was used to reveal changes in the membrane like opening of a fusion pore (Figure III-12A). Beginning from a reference state where the two vesicles are in contact one is able to analyze the image before and after fusion takes place, with the *a priori* knowledge that two membranes underwent fusion. The sequence of line profiles shown in the bottom left of Figure III-12 are for the period of time 250 μsec before the fusion event takes place. The line profiles consistently lie one on top of the other with the same characteristic features. Analyzing images surrounding the fusion event one begins to notice a change in the line profile (bottom right of Fig III-12) between two sequential pictures recorded at a time interval of 50 μsec. Comparison of the black and red line profiles indicates a shift in intensity indicating a change of approximately 1 μm. Fifty microseconds later the change is more pronounced on both sides of the line profile and there is a now a measurable shift in the boundary of the contact area. The shifts indicate that the adhered portion of the membrane, the gray value minimum, has been displaced over 5 μm towards the top of the image. This is consistent with an approximate shift in line profile maximum also of 5 μm. One more line profile is added, 200 μseconds later (300 μsec after the opening of the fusion pore), to demonstrate that the opening of the fusion

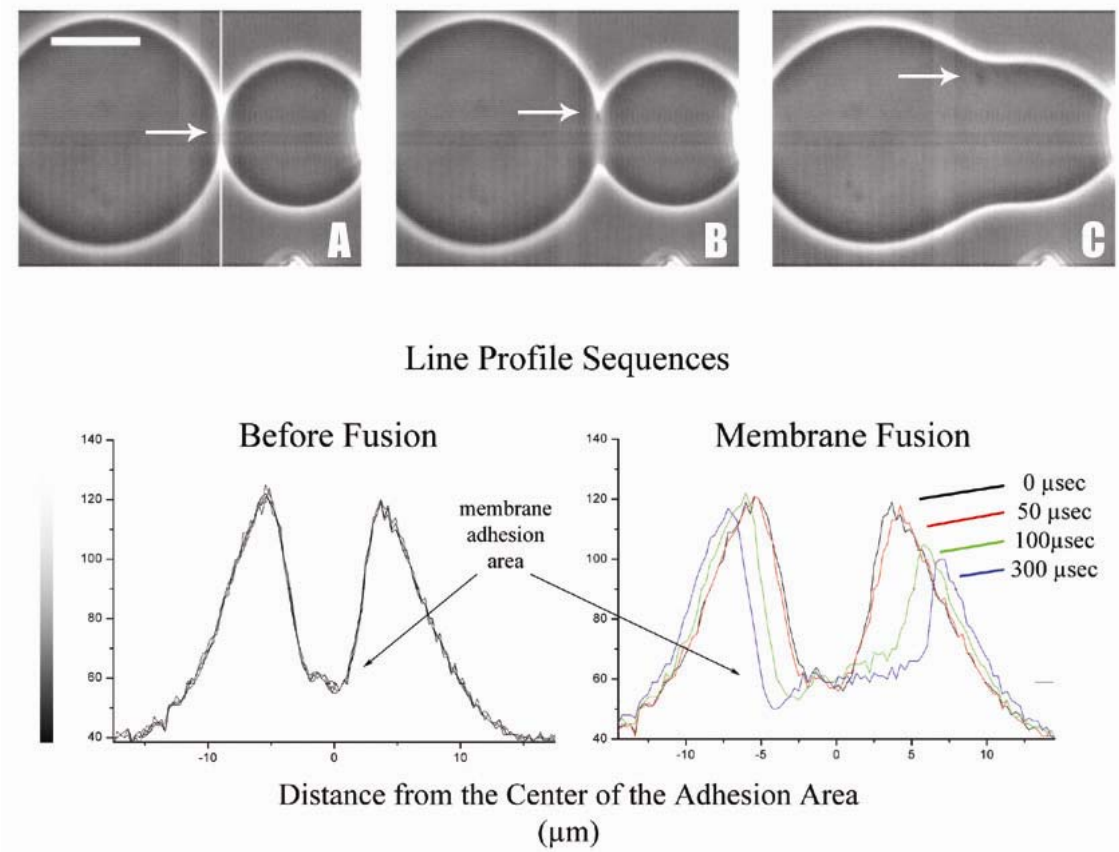

Figure III-12. Fusion Analysis: The micrographs above show three images from a recorded fusion event and the image analysis that accompanies it. In the three snapshots of a fusion event shown; image A, a reference state before the fusion takes place, indicates the contact area, the line profile used to analyze the opening of the fusion pore, and the scale bar equals 20 µm. Image B 300 microseconds later, the arrow follows the portion of the membrane area associated with the inter-membrane contact area. Here the fusion pore is already greater than 7 microns in diameter. Image C, shows fusion after 39 milliseconds, the arrow indicates the existence of a membrane defect associated with the inter-membrane contact area in A and B. (Below) The line profile sequences show, how the process of fusion unfolds. To the left line profiles are displayed for the 250 µsec leading up to the fusion event. To the right, are line profiles for four different times demonstrating fusion pore breaks. The arrows indicate changes in the position of the contact area before and after fusion occur.

pore continues irreversibly, and total membrane fusion occurs as a result of the 50µM $EuCl_3$ injection. Using line profile analysis of the fusion event we were able to trace how the opening of the fusion pore changes over time (Fig. IIII-13).

Of all of the fusion events recorded between isolated vesicles, complete opening of the fusion pore, that is that two spherical segments relaxed into one larger spherical segment, lasted less than a second. At normal recording rates, 24 frames per second (40 milliseconds between frames), that would result in a total of less than thirty points to analyze for a given fusion event. Whereas with the aid of the fast

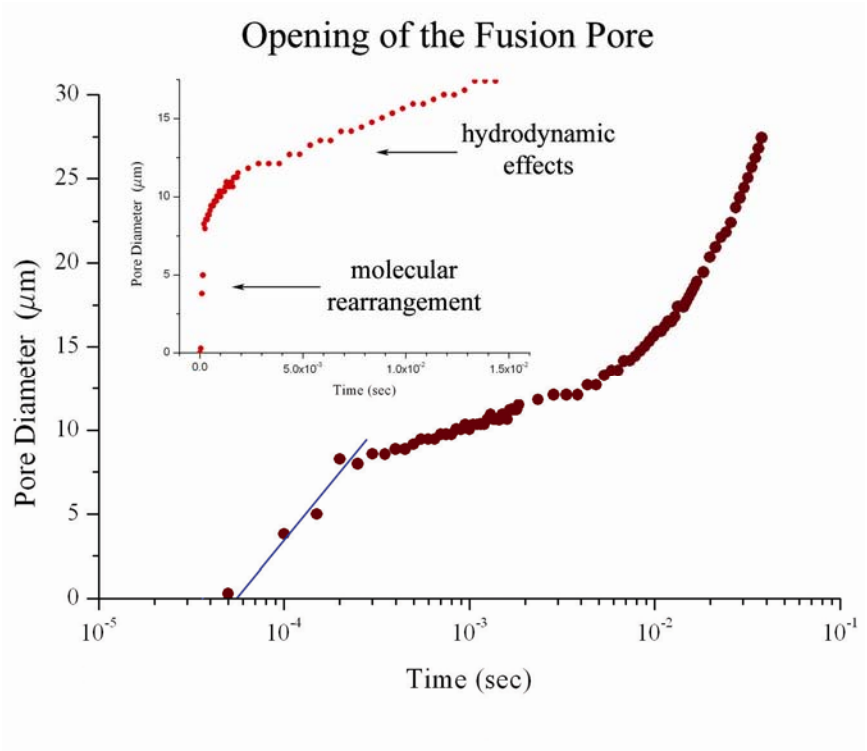

Figure III-13. Analysis of the Fusion Pore: Opening of fusion pore as revealed by analysis of the inter-membrane contact area line profiles. The diameter of the fusion pore is plotted as a function of time. From the main graph it is clear that there are two distinct processes involved in the opening of the fusion pore, one occurring on the order of microseconds and another on the order of milliseconds. Plotting the time on a logarithmic scale, allows us to extrapolate the data to a zero time where irreversible opening of the fusion pore occurs.

camera we have up to 20,000 frames per second per fusion event. By plotting the opening of the fusion pore on a logarithmic scale we are able to extrapolate the curve to reveal the time necessary before irreversible fusion of the two membranes occurs. We have found that time needed before irreversible opening of the fusion pore occurs is 40 μsec. Analysis of a fusion event allows us to describe the opening of the fusion pore with unprecedented accuracy, additionally on longer time scales more details associated membrane fusion are revealed.

Over the period of observation, one tenth of a second, the extent that the data can be analyzed, we are able to determine two distinct time scales associated with fusion of membranes (Figure III-13 inset). It can be concluded that on the short timescales, less than 500 μsec, the opening of the fusion pore is governed by molecular reorganization in the lipid bilayer and initial exchange of fluid between vesicle compartments. On times scales on the order of milliseconds the opening of the fusion pore is associated with outside forces applied to the membrane, such as the

surface tension when applied by the micropipette suction pressure, which are directly related to the costs associated with displacing the fluid surrounding the vesicle. The trend has been observed experimentally that longer times are required before vesicles with little or no tension are able to integrate the membrane defect associated with the vesicle contact area completely into the fused bilayer membrane, and thereby completing the fusion process. Measurements made with fluorescently labeled lipid showed no signs of hemifusion.

On paper the length of a fully stretched ligand-receptor inter-membrane complex is approximately 3nm, long enough to accommodate hydration layers associated with two lipid bilayers. This suggests that formation of a inter-membrane complex can exist in stable configuration between two vesicles. Observations made in this work on 2 component vesicles failed to make a connection between isotropic tension applied using micropipettes and fusion. Fusion events were observed using micropipettes, and in vesicles in a tensionless state free from micropipettes. These observations indicate the mechanism of fusion of the functionalized membranes may be defect driven, or a result of local perturbations to the membrane. Based on observations made the author puts forth the following suggestion as a mechanism for fusion of functionalized membranes.

Proposed Fusion Mechanism

- Ions induce nonspecific adhesion bilayer adhesion and multiple specific inter-membrane (one) ligand and (two) receptors complex formation.
- Desorption of ions from the bilayer act to reduce adhesion area and increase in undulation forces act to remove one or more receptors from an apposing bilayer at the edge of the adhesion area.
- Reinsertion of “unplugged” receptors plus remaining ions adsorbed on the membrane cause a defect in the adhered bilayers.
- Remaining stretched inter-membrane ligand receptor complexes over remaining adhesion area and membrane defect facilitates fusion pore opening.

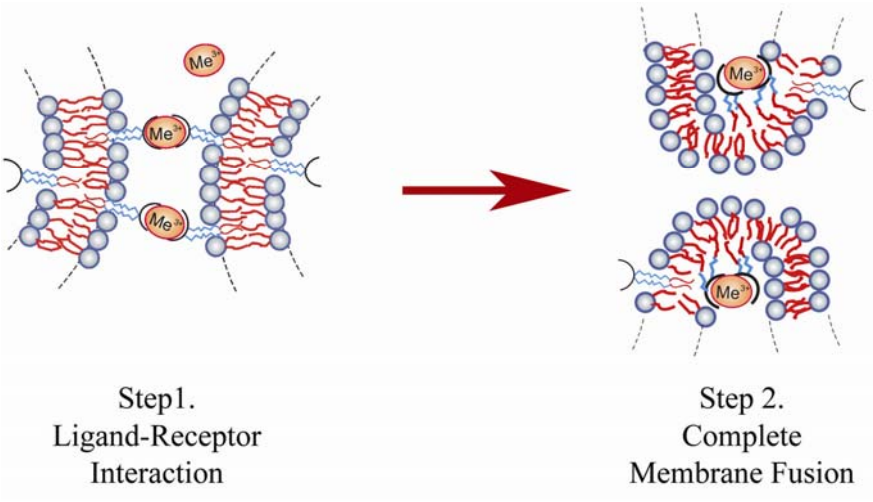

Figure III-14. Fusion Mechanism: The cartoons show the proposed structure of two steps in the events leading to the fusion of functionalized membranes, the close opposition of membrane through formation of ligand-receptor complex (left) and the opening of a fusion pore as fusion occurs.

3. Multi-Component Functionalized GUV's: Permeability

The multicomponent membranes behaved in a similar fashion to the pure Egg PC or functionalized vesicles, but also showed a different reaction to the presences of the $EuCl_3$. Indeed the addition of components such as cholesterol and PEG modified lipid changed the lipid bilayer properties and vesicle interaction behavior. In cases testing the interaction of multi-component membranes with vesicles in a closed packed environment, as well as in the vesicle isolation experiments, membrane fusion was not realized, but membrane failure was still observed. Additionally little adhesion was observed between the multicomponent membranes as a result of local injections of $EuCl_3$. Unexpectedly, one further response of the functionalized membrane to $EuCl_3$ was observed. We found an anomalous change in contrast between the interior and exterior of the vesicle as shown in Figure III-13. We find this behavior to be characteristic to the multicomponent GUV's in the presence of $EuCl_3$.

In the framework of membrane composition we have a good understanding of the origins of membrane failure. We attribute the lack of adhesion, and therefore membrane lack of fusion, to the presence of PEG2000-DMPC. It is well known that at low concentrations PEG modified lipids stabilize the membrane surface by providing a steric barrier to nonspecific interaction with opposing surfaces including the glass

substrate and other membranes (Woodle and Lasic 1992). As such the length of the PEG chains with 60 polyethylene oxide repeat units effectively neutralizes the interaction of two receptors in opposing bilayers and stabilizes the membranes against nonspecific interactions membranes leading to adhesion. The presence of cholesterol is known to reinforce the mechanical properties of membranes and prevent lysis of the bilayer (Needham and Nunn 1990). In this way we can expect fewer occurrences of membrane failure in the system.

The time dependent decrease in optical contrast as a result of 1mM europium (III) chloride injections, shown below, was particular to the multicomponent vesicles, and not often observed in measurements made on single component or two component vesicles. The micrographs show a collection of vesicles whose contrasts change as a result of $EuCl_3$.

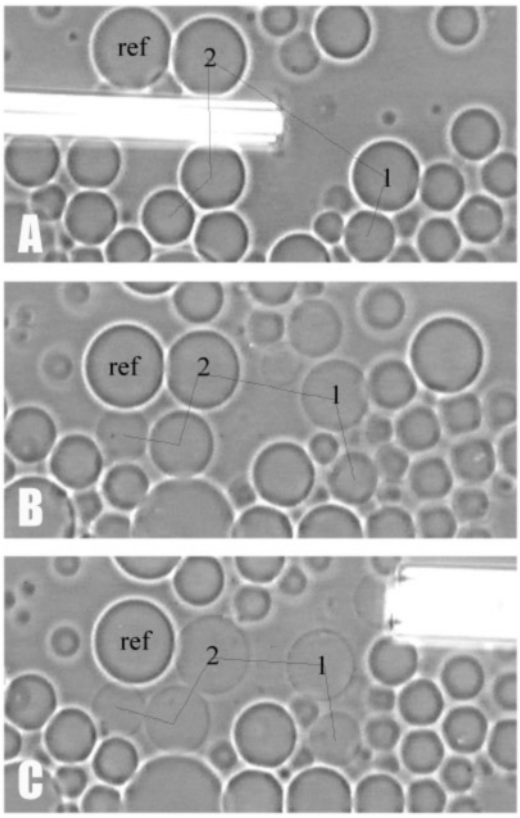

Figure III-15. Hyper-permeability: The long axis is 220 μm. The 3 micrographs show how the permeability of multicomponent membranes is increased in the presence of $EuCl_3$. A = 30 seconds after the injection, the injection pipette is shown . B = 150 seconds after the injection, contrast between glucose and sucrose is reduced. C = 270 seconds after the injection, contrast between vesicles is close to zero, indicating vesicle contents have completely mixed with the solution in the observation chamber. The line is used as an indicator to guide the reader to vesicles of interest

Based on the principle of phase contrast microscopy the optical contrast results from a difference in refractive index between sucrose and glucose solutions inside and outside of the vesicles respectively. A reduction in optical contrast can be related to equilibration of refractive index inside and outside the vesicle, which suggests a mixing of the vesicle contents with the surrounding solution. We use the changes in contrast to characterize the mixing of vesicle contents.

Changes in vesicle contents are detected using phase contrast microscopy. This is the same technique used to show that most of the volume was conserved during fusion of two vesicles described earlier. We analyze changes in the line profile intensity of the vesicles to monitor the fluid exchange over time. A comparison of decrease in the intensity of the halo surrounding the vesicles was compared with opposite changes in vesicle contrast, i.e. the bright halo with the dark interior. The graph below shows the measurement made for three different vesicles in Fig. III-13.

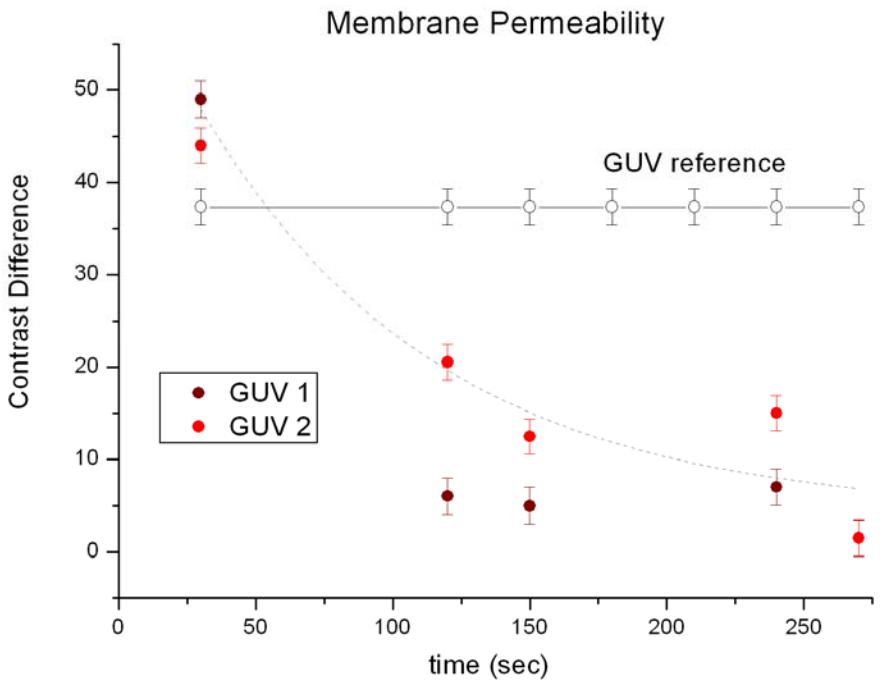

Figure III-16 Membrane Permeability Analysis: The graph shows the characterization of vesicles content mixing in three independent vesicles. Two vesicles underwent content mixing while the third is shown as a reference for comparison with the other two. The graph indicates that most of the content exchange occurs in the first 120 second after the injection is finished. The curve is used to guide the reader as to direction of the contrast change.

The graph shows the strongest decrease in the vesicle's contrast difference over the first 120 seconds in vesicles available for analysis. This can be attributed to the initial sucrose-glucose exchange. Over the next 3 minutes changes in contrast were negligible and within the error associated with the measurement. The results of the measurements are complimented by characterization of the vesicle radius to detect any change in total volume or membrane surface area due to membrane failure (not shown). Over the five minutes of contents mixing and observation the vesicles' radii remained constant with a measured value of ≈17 μm. A plausible explanation for the increased membrane permeability is the formation of pores in the membrane.

One can judge the size of the pore by the type of molecules that are passing through the bilayer and hydrophilic nature of the molecules in the bilayer. To minimize the exposure of the hydrophobic core to the exposure of the hydrophilic environment one can imagine a hydrophilic boundary with a radius of at least 3-4 nm, the thickness of the bilayer. Hydration layers must form at the surface of the bilayer, estimated from literature values the minimum depth of such a layer is 1 nanometer (Isra and Marra, Rand & Pasegian). That would result in a pore diameter greater than 2 nm. Pores with such a diameter should be sufficient to support a constant flux of most large molecules including sucrose or glucose molecules.

Comparison of the results obtained from the three levels of membrane complexity point us to our conclusion, and lead us to a mechanism for the formation of membrane pores. In the single component GUV's we suggest that ion-membrane interaction results in membrane lysis. Results obtained with two component functionalized membranes suggest the same effect with the additional possibility of membrane fusion through inter-membrane ligand-receptor complex formation. Pore formation in multicomponent membranes studied here can be explained with reference to the figure below, where one or more *intra*-membrane ligand-receptor complexes force the formation of a membrane pore.

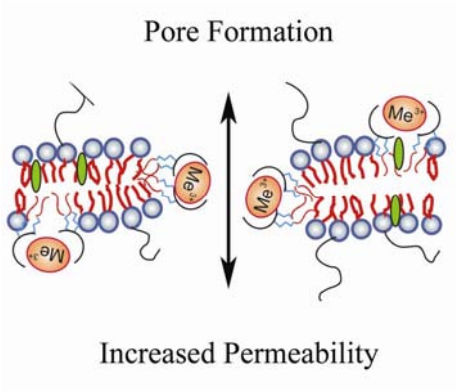

Figure III-17. Pore Stabilization: The illustration shows a possible mechanism of pore stabilization in multicomponent membranes (Cholesterol = green particles, PEG-lipid = long threads). Intra-membrane ligand receptor complex formation induces creation of a membrane pore. The reinforcing properties of cholesterol in the membrane stabilize against lysis and the flux of solution and hydration layers stabilize the pore against closing.

Based on these results one can expect a synergy between the processes involved with the ions interacting with the membrane and receptors. Perturbation is induced by ions close to the membrane, either due to adsorption of cations on the membrane and/or ligand-receptor complex formation. The membrane is stabilized against rupture due to the presence of additives such as cholesterol. Finally hydration of the pore opening stabilizes the pore from closing. The mechanism of pore formation and stabilization is not proven but based on the set of experiments performed we suggest the following mechanism as a hypothesis.

Proposed Mechanism of Membrane Pore Formation

- The presence of the adsorbed ions on the membrane induce a local tension
- 2:1 ligand-receptor also perturbs the membrane and acts to induce pore formation and transport of the ion across the lipid bilayer
- Cholesterol reinforces the membrane against lysis
- Stable pore formation occurs as a balance of membrane forces acting to open the membrane and counter forces acting to close the pore.

Using micromolar concentrations we have investigated the interaction of four different electrolytes with pure and functionalized lipid bilayers. Based on the results we have identified four classes of behavior dependent on membrane composition. First, interaction of europium (III) chloride induces membrane failure in both classes

of giant unilamellar vesicles regardless of functionality or the presence of additives such as cholesterol and steric spacers like PEG-lipid. Next, as a result of local injections interaction of europium (III) chloride ions at the water-lipid bilayer interface leads to reversible inter-membrane adhesion and bilayer adhesion to the glass substrate. The two adhesion processes are also observed in functionalized vesicles without steric spacers. We have determined that this adhesion is a result of non specific interaction not a result of specific ligand-receptor interaction. Results observed to be a product of ligand receptor interaction were discovered to be dependent on membrane composition. Two component membranes containing lipid and amphiphilic receptors lead to the observation of complete membrane fusion which, within experimental error, appeared to be lossless. Finally, we move towards a more natural system, enriching the bilayer by adding a modified lipid as a steric spacer and strengthening the bilayer with cholesterol we found that the ligand receptor interaction produced a hyper-permeable bilayer which was able to easily able to transport large molecules such as sucrose or glucose across the bilayer. Transport of large molecules without membrane surface area change was rationalized as a product of formation of pores in the membrane.

Due to the difficulties with the system, particularly the low number of vesicles fusion events observed per measurement ($\leq$ 10 %), we were able to develop a hypothesis to describe the fusion process in our system. As was shown throughout this work the collective behavior of europium (III) chloride interaction with lipids in the membrane and/or receptors can be quite complex, often involving the superposition of several processes, and therefore it is difficult to disentangle individual mechanisms that induce pore formation and fusion. In reality the results have shown membrane stabilities and instabilities are a synergistic effect of many different factors. In this way we have laid the groundwork to investigate more detailed features of this complex system by quantitatively measuring changes in fundamental properties of the bilayer and to optimize changes that lead to fusion and increased membrane permeability. By investigating membranes with various levels of complexity we were able to observe the response of the ligands in different membrane environments and end up qualitatively describing a variety of distinct processes induced by europium (III) chloride. While the conclusions drawn about the ligand-receptor interactions

inducing membrane fusion and hyper-permeability the are still not definitively proven, we have gained a more comprehensive picture of the affects induced via ligand-receptor interactions and put ourselves in a position to the test proposed hypothesis.

IV. Conclusion & Outlook

We use sub-microscopic large unilamellar vesicles (LUV's), and giant unilamellar vesicles (GUV's) which are optically accessible, to study the effects of specific ligand-receptor interaction and understand the physical aspects associated with interactions of lipid bilayers. We investigate the impact of ions at membrane surfaces and how adsorption of multivalent cations onto the lipid bilayer mediates intermembrane recognition and changes membrane properties. Furthermore we functionalize the membranes with ß-diketone and bipyridine receptors to induce specific ligand-receptor recognition. As such we are able to understand how ligand (cation)-receptor interactions change the membrane properties and lead to hyper-permeable membranes and complete fusion between two lipid bilayers.

In this work we are interested in understanding the way the lipid bilayer interaction is affected through specific molecular recognition. To do this we studied the effect of Egg PC LUV's and functionalized LUV's in the presence of different electrolyte solutions using isothermal titration calorimetry. The measurements showed that divalent electrolytes, $NiCl_2$ and $CuCl_2$, interact weakly, if at all, with single component vesicle membranes. The measurement was comparable to the interaction associated mixing of europium (III) chloride with aqueous glucose solution, i.e. the medium without vesicles. In contrast there was significant endothermic interaction as a result of the interaction between the vesicle membrane and electrolytes like $EuCl_3$, and $GdCl_3$. We attempted to gain a molecular understanding of the processes involved through a comparison of the results obtained for interaction of $EuCl_3$ in different systems, i.e. pure Egg PC versus membranes functionalized with ß-diketone receptors. Interaction between the Egg PC bilayer and the $EuCl_3$ is characterized by entropic interaction which results in a molar enthalpy ΔH measured to be 0.1 kcal/mole, and an equilibrium constant K= 31±4 mM^{-1}. With the presence of 0.5 % (mole) ß-diketone in the membrane, interaction was exothermic and characterized by ΔH = 126±5 kcal/mole and K= 26 ± 4 mM^{-1}. The data obtained suggest the formation of a ligand receptor complex between one Eu^{3+} and two ß-diketone receptors.

The ITC study was complemented with light scattering measurements that revealed negligible changes in mean vesicle size but measurable changes in vesicle size distribution. Measurements of vesicle size revealed that very little change in mean vesicle diameter occurred as a result of the addition of electrolyte. On the other hand there was a measurable change in the distribution of vesicle radii as a result of injection of electrolyte into the vesicle dispersion. On average the changes in vesicle size distribution measured were 20%, but change in LUV size distribution was shown to be independent of the millimolar concentration of the electrolytes used, and membrane composition, i.e. functional LUV's in comparison with Egg PC LUV's. We conjecture that the change in size distribution results from in the case of decrease in radii, membrane failure and volume leakage, or in the case of increasing vesicle radii, adhesion or fusion. Due to the simplicity of the system we can attribute the changes in size distribution to the interaction of the ions with the membrane leading to the above mentioned effects.

Small Vesicles Summary

- Interaction energies measured with ITC resulting in an endothermic signal are a binding due to adsorption of ions on the membrane, and or in a layer close to the membrane.
- Large exothermic binding signal is suspected to be a result of specific ligand-receptor involving one Eu^{3+} and two ß-diketone receptors.
- Changes in vesicle size distribution are a result of membrane failure, or inter-vesicle adhesion in the case of ion-membrane interaction in EPC LUV's. In the case of functionalized membranes change in size distribution is thought to include membrane fusion as well. All predictions were found to be consistent with measurements performed on GUV's described below.

With the results mentioned above, we turn our attention to macroscopic studies of GUV's using optical microscopy. We are interested in factors that were measurable with the ITC. Since the ITC results lead to the conclusion that divalent ions do not interact strongly with the membrane we chose to focus our attention to studies with membranes and europium (III) chloride. Using the combination of micropipette manipulation and optical microscopy we are able to characterize the system through direct observations in real time. By varying the membrane composition we aimed to directly characterize different effects of ion-membrane and

ligand (cation)-receptor interactions based on the properties of the membrane additives. What we found is that the concentration of electrolyte at the membrane interface acts to induce a non-specific adhesion between two membranes. In two component membranes, i.e. membranes with ß-diketone receptors, the interaction of europium (III) chloride in the framework of specific ligand (cation)-receptor interaction acted to induce fusion. In multi-component membranes europium (III) chloride had a dramatic effect on the permeability of the membrane. From the observations one can compare the systems of single, bi- and multi-component and membranes and extrapolate results to come up with a coherent mechanism that explains the differences in the results.

Giant Vesicles Summary

- Nonspecific interaction between the trivalent cations and the PC membrane can explain adhesion of both single and bi-component vesicles in presence of electrolytes.
- Membrane failure results from a local tension induced by nonspecific ion-membrane interaction.
- Membrane permeability is a result of intra-membrane ligand (cation)-receptor interaction.
- Fusion of vesicles results from inter-membrane ligand (cation)-receptor interaction.

Based on the description above, measurements made on both LUV's and GUV's are in agreement with one another. The measurements made up to now show promise in development of a system of interacting membranes based on highly specific recognition. Membrane stability is a primary obstacle to successful characterization. One must understand how the ions are interacting with the lipid bilayer to induce membrane rupture, in order to prevent it. With more stable membranes we can develop a better understanding of the specific properties that will promote ligand (cation)-receptor interaction over ion membrane interactions. With this characterization achieved we will be able to proceed towards optimization of the processes of interest, namely membrane fusion and permeability. In that way we will have developed understanding of a functional system acting on the basis of highly specific membrane recognition.

In the foreseeable future a number of experiments can be envisaged to help elucidate the interaction of the ions with the membranes using the existing large and

giant vesicle systems.

Potential Measurements

LUV's

- Zeta potential measurements on neutral and functionalized vesicles in the presence of ions can be used to determine how the membrane surface potential changes as a result of ions adsorbed on the membrane.
- Photophysical properties of the LUV suspension such as absorbance and fluorescence are affected by ligand-receptor complex formation. One can determine at what electrolyte concentration these changes occur.
- Dynamic light scattering measurements can be performed as a function of ion concentration to determine when changes in membrane sizes begin to occur.
- X-ray or neutron scattering experiments can be applied to determine differences in inter-membrane spacing as a result of ligand-receptor interaction.

GUV's

- Macroscopic changes in vesicle area and tension can be studied to determine the collective affect of adsorption of ions on the phospholipid membrane.
- In an attempt to visualize the fluorescence as a result of ligand-receptor complex formation, one can perform measurements using the D_2O in solution to reduce quenching of Eu^{3+} in the presence of H_2O.
- Optimization of the fusion process through addition of curvature stabilizing lipids like PE's in order to study the fusion pore opening in more detail.
- Detailed characterization of the membrane pore formation observed in complex membranes using micropipettes.
- Use of different ligands or incorporation of proteins into model membranes to compare differences in process of membrane fusion.

Acknowledgements

There are a number of people I would like to thank for their support during my studies here in Germany. Primarily I am indebted to; Prof. Lipowsky, for giving me the financial and time support to complete this work. Rumiana Dimova, for her guidance and supervision through my studies at the institute, and Valerie Marchi-Artzner, for the consultation during this thesis, and providing the amphiphilic receptors used in this study.

A little closer to home, I would like to thank the people in the theory department who helped me along the way. Through discussions about experimental results or just any ideas I had, they include, and I am indebted to; Julian, Vesko, Connie, Said, Karin, Pavel, Janine, Jan, last and certainly not least, Antje. Without their support I most likely would not have made it this far. You all deserve a big pat on the back for all that you have done for me.

Outside of these people, I have to say thank you to the people from other departments, the Colloid and Interfaces, at the institute, especially Miles, Ralf, Charl and James for their useful discussions, and relief from the pains of Glom, and reading this thesis first.

V. Bibliography

Alberts, B., A. Johnson, et al. (2001). Molecular Biology of the Cell. New York, New York, Garland Science.

Altenbach, C. and J. Seelig (1984). "Ca^{2+} Binding to Phosphatidylcholine Bilayers as Studied by Deutrium Magnetic Resonance. Evidence for the Formation of a Ca^{2+} Complex with Two Phospholipid Molecules." Biochemistry **23**(17): 3913-3920.

Bauer, H., J. Blanc, et al. (1964). "Octacoordinate Chelates of Lanthanides. Two Series Compounds." J. Am. Chem. Soc. **86**: 5125-5131.

Duportail, G. and P. Lianos (1996). Fluoresence Probing of Vesicles Using Pyrene and Pyrene Derivatives. Vesicles. M. Rosoff. New York, Marcel Dekker, Inc. **62:** 373-439.

Duzgunes, N., J. Bentz, et al. (1988). "La^{3+} Induced Fusion of Phosphatidylserine Liposomes> Close approach, Intermembrane Intermediates and the Electrostatic Surface Potential." Biophys. J. **53**: 593-607.

Duzgunes, N., J. Wilschut, et al. (1983). "Aggregation and Fusion of Phospholipid Vesicles." Progress in Surface Science **13**: 1-124.
Evans, E. A. (1980). "Analysis of Adhesion of Large Vesicles to Surfaces." Biophys. J. **31**: 425-432.

Evans, E. A. (1980). "Minimum Energy Analysis of Membrane Deformation Applied to Pipet Aspiration and Surface Adhesion of Red Blood Cells." Biophys. J. **30**: 265-284.

Evans, E. A. and M. Metcalfe (1984). "Free Energy Potential for Aggregation of Giant, Neutral Lipid Bilayer Vesicles by Van der Waals Attraction." Biophys. J. **46**: 423-426.

Evans, E. A. and A. V. Parsegian (1983). "Energetics of Membrane Deformation and Adhesion in Cell and Vesicle Aggregation." Annals New York Academy of Sciences: 13-33.

Harbich, W. and W. Helfrich (1979). "Alignment and Opening of Giant Lecithin Vesicles by Electric Fields." Z. Naturforschung **34a**: 1063-1065.

Heerklotz, H. and J. Seelig (2000). "Titration Calorimetry of Surfactant-Membrane Partitioning and Solubization." Biochemica et Biophysica Acta **1508**: 69-85.

Helfrich, W. (1973). "Elastic Properties of Lipid Bilayers:Theory and Possible Experiment." Z. Naturforschung **28 c**: 693-703.

Heuvingh, J., F. Pincet, et al. (2004). "Hemifusion and fusion of giant vesicles induced by reduction of inter-membrane distance." European Physical Journal E.

Israelachvili, J. N. (2002). Intermolecular and Surface Forces. London, Academic Press.

Jahn, R. and H. Grubmüller (2002). "Membrane Fusion." Current Opinion in Cell Biology **14**: 488-495.

Jahn, R., T. Lang, et al. (2003). "Membrane Fusion." Cell **112**: 519-533.

Kozlov, M. M. and V. S. Markin (1983). "Possible Mechanism of Memebrane Fusion." Biofizka **28**: 255-261.

Lasic, D. D. (1993). Liposomes: From Physics to Applications. Amsterdam, Elsevier Science.

Lee, J. and B. R. Lentz (1997). "Evolutionof Lipidic Structures During Model Membrane Fusion and the Relation of This Process to Cell Membrane Fusion." Biochemistry **36**(21): 6251.

Lehn, J.-M., N. Sabbatini, et al. (1993). "Luminescent Lanthanide Complexes as Photochemical Supramolecular Devices." Coordination Chemistry Reviews **123**: 201-228.

Lehrman, R. and J. Seelig (1994). "Adsorption of Ca^{2+} and La^{3+} to bilayer membranes: Measurement of Adsorption Enthalpy and Binding Constant with Titration Calorimetry." Biochemica et Biophysica Acta **1189**: 89-95.

Lentz, B., V. Malinin, et al. (2000). "Protein Machines and Lipid Assemblies: Current Views of Cell Membrane Fusion." Current Opinion in Structural Biology **10**: 607-615.

Luisi, P. L. and P. Walde, Eds. (2000). Giant Vesicles. Perspectives in Supramolecular Chemistry. West Sussex, John Wiley and Sons.

Marchi-Artzner, V., M.-J. Brienne, et al. (2004). "Selective Complexation and Transport of Europium Ions at the Interface of Vesicles." Chem. Eur. J. **10**: 2342-2350.

Markin, V. S. and J. P. Albanesi (2002). "Membrane Fusion: Stalk Model Revisited." Biophys. J. **82**: 693-712.

Marra, J. and J. N. Israelachvili (1985). "Direct measurements of Forces between Phosphatidylcholine and Phosphatidylethanolamine Bilayers in Aqueous Electrolyte Solutions." Biochemistry **24**: 4608-4618.

Needham, D. and R. S. Nunn (1990). "Elastic deformation and Failure in Lipid Bilayer Membranes Containing Cholesterol." Biophys. J. **58**: 997-1009.

Needham, D. and D. V. Zhelev (1996). The Mechanochemistry of Lipid Vesicles Examined by Micropipet Manipulation Techniques. Vesicles. M. Rosoff. New York, Marcel Dekker, Inc. **62:** 373-439.

Pantazatos, D. P. and R. C. MacDonald (1999). "Directly Observed Membrane Fusion Between Oppositely Charged Phospholipid Bilayers." Journal of Membrane Biology **170**: 27-38.

Papahadjopoulos, D., G. Poste, et al. (1973). "Fusion of mammalian cells by unilamellar lipid vesicles: Influence of lipid surface charge, fluidity and cholesterol." Biochimica et Biophysica Acta (BBA) - Biomembranes **323**(1): 23-42.

Papahadjopoulos, D., W. J. Vail, et al. (1977). "Studies on membrane fusion. III. The role of calcium-induced phase changes." Biochimica et Biophysica Acta (BBA) - Biomembranes **465**(3): 579-598.

Rand, R. P. and A. V. Parsegian (1989). "Hydration forces between phospholipid bilayers." Biochemica et Biophysica Acta **988**: 351-376.

Reeves, J. P. and R. M. Dowben (1968). "Formation and Properties of Thin-walled Phospholipid Vesicles." Journal of Cell Physiology **73**: 49-60.

Seifert, U. (1997). "Configurations of Fluid Membranes and Vesicles." Advances in Physics **46**(1): 13-137.

Tamm, L., J. Crane, et al. (2003). "Membrane Fusion: a Structural Perspective on the Interplay of Lipids and Proteins." Current Opinion in Structural Biology **13**: 453-466.

Tanford, C. (1980). The Hydrophobic Effect. New York, Wiley.

Van Zanten, J. H. (1996). Characterization of Vesicles and Vesicle Dispersions via Scattering Techniques. Vesicles. M. Rosoff. New York, Marcel Dekker, Inc. **62:** 373-439.

Wimley, W. C. and T. E. Thompson (1990). Biochemistry **29**: 1296-1303.

Woodle, M. C. and D. D. Lasic (1992). "Sterically Stabilized Liposomes." Biochemica et Biophysica Acta **1113**: 171-199.